SPEG Controls Calcium Re-Uptake into the Sarcoplasmic Reticulum Through Regulating SERCA2a by Its Second Kinase-Domain

Quan, Chao; Li, Min; Du, Qian; Chen, Qiaoli; Wang, Hong; Campbell, David G.

Published in:
Circulation Research

DOI:
10.1161/CIRCRESAHA.118.313916

Publication date:
2019

Document Version
Peer reviewed version

Accepted Manuscript version of Quan, C, Li, M, Du, Q, Chen, Q, Wang, H, Campbell, DG, Fang, L, Xue, B, MacKintosh, C, Gao, X, Ouyang, K, Wang, H & Chen, S 2018, 'SPEG Controls Calcium Re-Uptake into the Sarcoplasmic Reticulum Through Regulating SERCA2a by Its Second Kinase-Domain', Circulation Research. https://doi.org/10.1161/CIRCRESAHA.118.313916

SPEG controls calcium re-uptake into the sarcoplasmic reticulum through regulating SERCA2a by its second kinase-domain

Chao Quan[1,6], Min Li[1,6], Qian Du[1], Qiaoli Chen[1], Hong Wang[2], David Campbell[3], Lei Fang[4], Bin Xue[4], Carol MacKintosh[5], Xiang Gao[1], Kunfu Ouyang[2], Hong Yu Wang[1] and Shuai Chen[1]*

[1]State Key Laboratory of Pharmaceutical Biotechnology, Department of Cardiology, Nanjing Drum Tower Hospital, The Affiliated Hospital of Nanjing University Medical School, Model Animal Research Center, Nanjing University, Nanjing, 210061, China

[2]Key Laboratory of Chemical Genomics, School of Chemical Biology and Biotechnology, Peking University, Shenzhen 518055, China

[3]MRC Protein Phosphorylation and Ubiquitylation Unit, School of Life Sciences, University of Dundee, Dundee DD1 5EH, Scotland, U.K.

[4]School of Medicine, Nanjing University, Nanjing, 210061, China

[5]Division of Cell and Developmental Biology, School of Life Sciences, University of Dundee, Dundee DD1 5EH, Scotland, U.K.

[6]Co-first author

* corresponding author

Running title: Regulation of SERCA2 by SPEG

Keywords: SPEG, SERCA, phosphorylation, calcium, heart.

Correspondence to: Shuai Chen (schen6@163.com or chenshuai@nicemice.cn), State Key Laboratory of Pharmaceutical Biotechnology and MOE Key Laboratory of Model Animal for Disease Study, Model Animal Research Center, Nanjing Biomedical Research Institute, Nanjing University, Pukou District, Nanjing, 210061, China

Abbreviations: ER, endoplasmic reticulum; MCM, MerCreMer; SERCA2a, Sarcoplasmic/endoplasmic reticulum calcium ATPase 2a; SK, serine/threonine (Ser/Thr) kinase; SR, sarcoplasmic reticulum; SPEG, striated muscle preferentially expressed protein kinase.

ABSTRACT

Rationale: Striated muscle preferentially expressed protein kinase (SPEG) has two kinase-domains and is critical for cardiac development and function. However, it is not clear how these two kinase-domains function to maintain cardiac performance.

Objective: To determine the molecular functions of the two kinase-domains of SPEG.

Methods and Results: A proteomics approach identified sarcoplasmic/endoplasmic reticulum calcium-ATPase 2a (SERCA2a) as a protein interacting with the second kinase-domain but not the first kinase-domain of SPEG. Furthermore, the second kinase-domain of SPEG could phosphorylate Thr^{484} on SERCA2a, promote its oligomerization and increase calcium re-uptake into the sarcoplasmic/endoplasmic reticulum in culture cells and primary neonatal rat cardiomyocytes. Phosphorylation of SERCA2a by SPEG enhanced its calcium transporting activity without affecting its ATPase activity. Depletion of *Speg* in neonatal rat cardiomyocytes inhibited SERCA2a Thr^{484} phosphorylation and SR calcium re-uptake. Moreover, over-expression of $SERCA2a^{Thr484Ala}$ mutant protein also slowed SR calcium re-uptake in neonatal rat cardiomyocytes. In contrast, domain-mapping and phosphorylation analysis revealed that the first kinase-domain of SPEG interacted and phosphorylated its recently-identified substrate junctophilin-2 (JPH2). An inducible heart-specific *Speg* knockout mouse model was generated to further study this SPEG-SERCA2a signal nexus *in vivo*. Inducible deletion of *Speg* decreased SERCA2a Thr^{484} phosphorylation and its oliogomerization in the heart. Importantly, inducible deletion of *Speg* inhibited SERCA2a calcium transporting activity and impaired calcium re-uptake into the SR in cardiomyocytes, which preceded morphological and functional alterations of the heart and eventually led to heart failure in adult mice.

Conclusion: Our data demonstrate that the two kinase-domains of SPEG may play distinct roles to regulate cardiac function. The second kinase-domain of SPEG is a critical regulator for SERCA2a. Our findings suggest that SPEG may serve as a new target to modulate SERCA2a activation for treatment of heart diseases with impaired calcium homeostasis.

INTRODUCTION

Calcium entry into and release from the sarcoplasmic reticulum (SR) are pivotal processes during excitation-contraction coupling to control the contraction and relaxation cycle of cardiac muscle, whose dysregulation causes cardiac dysfunction and is directly linked to cardiomyopathy and heart failure [1]. Restoration of cardiac calcium homeostasis is an attractive strategy to treat heart disease associated with calcium dysregulation, which requires a comprehensive understanding of how this process is regulated.

Sarcoplasmic/endoplasmic reticulum calcium ATPase 2a (SERCA2a) in cardiomyocytes is a critical ATPase for re-uptake of calcium from the cytosol back into the SR during muscle relaxation [2]. Decreased expression and activity of SERCA2a impedes calcium re-uptake into the SR and impairs muscle contraction and relaxation, which is a hallmark of heart failure [3]. Multiple mechanisms have been identified to regulate SERCA2a activity in cardiomyocytes including interaction with a regulatory protein, phospholamban (PLB) [3], and post-translational modifications such as SUMOylation [4], nitration [5] and glutathiolation [6]. SERCA2a can be phosphorylated on Ser^{38} by SR-associated Ca^{2+}/calmodulin-dependent protein kinase (CaMK) [7], whose physiological relevance in regulation of calcium re-uptake is still to be determined. There is also evidence that SERCA2a forms functional oligomers in cardiac muscle [8-10], analogous to the functional dimeric unit of SERCA1 in skeletal muscle [11].

Striated muscle preferentially expressed protein kinase (SPEG) is a member of the myosin light chain kinase (MLCK) subgroup of CaMK Ser/Thr protein kinase family [12]. It is mainly found in the skeletal muscle and heart, and has two serine/threonine (Ser/Thr) kinase (SK) domains in its C-terminal region, referred to as SK1 and SK2 [12]. Its deletion in mice impairs cytoskeleton function in cardiomyocytes in the developing heart and causes dilated cardiomyopathy in mouse embryos. Consequently, mice with whole-body deletion of SPEG die neonatally probably due to cardiac dilatation during heart development [13]. Neonatal death in these mice can be rescued by administration of cardiac progenitor cells [14]. Moreover, cardiac-specific deletion of SPEG in adult mice also caused dilated cardiomyopathy and resulted in heart failure [15]. Human patients carrying homozygous or compound-heterozygous SPEG mutations also develop dilated cardiomyopathy [16]. Besides its effects in the heart, deficiency of SPEG can also cause centronuclear myopathy in skeletal muscle in mice as well as in human [16]. These studies demonstrate a critical role of SPEG in striated muscle and also heighten the needs to elucidate the underlying mechanisms. Being a member of the MLCK subgroup, the SK1 of SPEG exhibits higher similarity with other kinases within this subgroup than does the SK2 [12]. So far, it remains unclear how these two kinase domains of SPEG function to maintain cardiac performance.

In this study, we identified SERCA2a as a protein that interacted with the SK2 of SPEG in the heart, and demonstrated a critical role of the SK2 of SPEG in regulating calcium re-uptake into the SR through phosphorylation and oligomerization of SERCA2a.

MATERIALS AND METHODS

Materials

Protein G-Sepharose was purchased from GE Healthcare (Little Chalfont, Buckinghamshire, UK). Precast NuPAGE® Bis-Tris gels and the crosslinker dithiobis[succinimidyl propionate] (DSP)

were from Thermo Fisher Scientific (Waltham, MA, USA). All other chemicals were from Sigma-Aldrich (Shanghai, China) or Sangon Biotech (Shanghai, China).

Antibodies

The rabbit antibody against SPEG (Cat No. 12472-RP02) was from Sino Biologicals (Beijing, China). The rabbit antibody against SERCA2a (Cat No. 13985-1-AP) was from Proteintech (Wuhan, China). The mouse antibody against SERCA2a (Cat No. MA3-910) was from Thermo Fisher Scientific. The goat antibody against SERCA2a (Cat No. sc-8095), and the HA (Cat No. sc-805) and GFP (Cat No. sc-8334) antibodies were from Santa Cruz (Dallas, Texas, USA). The PLB antibody (Cat No. ab126174) and triadin antibody (Cat No. ab2870) were from Abcam (Cambridge, UK). The pSer^{16}-PLB antibody (Cat No. 07-052) was from Merck Millipore (Danvers, MA, USA). The phospho-Ser antibody (Cat No. 37430) and phospho-Thr antibody (Cat No. 37420) were from Qiagen (Hilden, Germany). The GAPDH (Cat No. G8795) and Flag (Cat No. F9291) antibodies were from Sigma. GFP-Trap®-agarose (GFP-binder) was from Chromotek (Planegg-Martinsried, Germany).

Molecular biology

The mouse SPEG cDNA or human SERCA2a cDNA were cloned into the vectors pcDNA5-FRT/TO-GFP or pcDNA5-FRT/TO-HA or pcDNA5-FRT/TO-Flag for expression in mammalian cells, or cloned into the pGEX6P vector for protein expression in *E. coli*. Fragmentation and point mutation of SPEG or SERCA2a were carried out using standard procedures. The sequence contexts of mutated sites on SERCA2a are: LMKKEF**t**LEFSRD (Thr^{484} in lower-case bold), EFTLEF**s**RDRKSM (Ser^{488} in lower-case bold), FSRDRK**s**MSVYCT (Ser^{493} in lower-case bold), RDRKSM**s**VYCTPN (Ser^{495} in lower-case bold), SMSVYC**t**PNKPSR (Thr^{499} in lower-case bold), CTPNKP**s**RTSMSK (Ser^{504} in lower-case bold), THIRVG**st**KVPMTS (Ser^{531}/Thr^{532} in lower-case bold), VKQKIM**s**VIREWG (Ser^{546} in lower-case bold). All DNA constructs were sequenced by Life Technologies (Shanghai, China).

Generation of *Speg*$^{f/f}$ and *Speg* knockout mice

The *Speg* knockout-first ES cells (Cell line: JM8.N4; Clone: EPD0180_2_A07) were obtained from Knockout Mouse Project (KOMP) Repository (University of California Davis and Children's Hospital Oakland Research Institute, USA), and used to generate the *Speg*$^{f/f}$ mice, in which the ninth exon of *Speg* was flanked by *loxP* sites. The *Speg*$^{f/f}$ mice were backcrossed to C57Bl/6J background for at least 5 generations before experiments. The Myh6-MerCreMer (Myh6-MCM) [20] and αMHC-Cre [17] mice on a C57Bl/6J background, were bought from the Nanjing Biomedical Research Institute of Nanjing University, and mated with the *Speg*$^{f/f}$ mice to obtain cardiac specific *Speg* inducible knockout mice and cardiac specific *Speg* knockout mice, respectively.

Mouse breeding, husbandry, and tamoxifen induction

All mouse procedures used in this study were approved by the Ethics Committee at Model Animal Research Center of Nanjing University. Minimal numbers of animals were used in the study, which could still allow for generation of statistically meaningful results. Mice were maintained under specific pathogen free conditions with a light/dark cycle of 12 h.

As for inducible cardiac-specific knockout mice, *Speg*$^{f/f}$ X *Speg*$^{f/f}$/Myh6-MCM mating was set up to generate *Speg*$^{f/f}$ (control mice) and *Speg*$^{f/f}$/Myh6-MCM (cardiac-specific *Speg* inducible knockout mice). As for cardiac-specific knockout mice, *Speg*$^{f/f}$ X *Speg*$^{f/f}$/αMHC-Cre mating was set up to generate *Speg*$^{f/f}$ (control mice) and *Speg*$^{f/f}$/αMHC-Cre (cardiac-specific *Speg* knockout mice).

The *Speg* flox allele was genotyped via PCR using the following primers: 5'-CTCAGTCATAGCAGCATCAC-3' and 5'-ATCCAAAGCCAGGTTTACCCC-3'. The *Cre* locus was genotyped via PCR using the following primers: 5'-AATGCTTCTGTCCGTTTGC-3' and 5'-ACCAGAGTCATCCTTAGCG-3'.

For tamoxifen induction, mice were intraperitoneally administered with 20 mg/kg/d tamoxifen for five consecutive days.

Tissue lysis and measurement of protein concentration

After harvest, mouse tissues were snap-frozen in liquid nitrogen, and homogenized in lysis buffer using a Polytron homogenizer (Kinematica, Luzern, Switzerland) as previously described [30]. Homogenates were further lysed on ice for 30 min, and tissue debris was removed through centrifugation. Protein concentrations were determined using Bradford reagent (Thermo Scientific).

Immunoprecipitation and immunoblotting

Immunoprecipitation was carried out as previously described [30]. Briefly, tissue or cell lysates were mixed with the antibody-coupled protein G-Sepharose or GFP-binder (ChromoTek GmbH, Planegg-Martinsried, Germany), and incubated overnight at 4^{o}C. Thereafter, non-specific binding proteins were removed through washing, and immunoprecipitates were eluted off from the resins in SDS sample buffer.

For SERCA2a dimerization assay via immunoblotting, cell or tissue lysates were denatured in SDS sample buffer without reducing agents at room temperature for 15 min. In all the other immunoblotting assays, samples were denatured in SDS sample buffer containing reducing agents at 95°C for 15 min. After separation via SDS-PAGE, lysates or immunoprecipitates were immunoblotted onto nitrocellulose membranes. Membranes were then sequentially incubated with primary antibodies and horseradish-peroxidase-conjugated secondary antibodies. After incubation with ECL substrates (GE Healthcare, UK), chemiluminescence signals were recorded using a gel documentation system (Syngene, UK). Images of immunoblots were quantified using ImageJ. When protein phosphorylation was quantified, signals for phosphorylated proteins were normalized with corresponding total proteins. When total proteins were quantified, their signals were normalized with internal loading controls.

Mass-spectrometry

Immunoprecipitated proteins were electrophoretically separated in precast NuPAGE® Bis-Tris gels. After stained with Commassie dye, protein bands were excised and digested with trypsin. The resultant peptides were analysed by LC-MS on an LTQ-Orbitrap (Thermo Finnigan) mass spectrometer coupled to a Dionex 3000 nano liquid chromatography system as described previously [31].

Generation of site-specific pThr^{484}-SERCA2a antibody

The antibody that recognizes phosphorylated Thr^{484} site in SERCA2a was raised in rabbit against the following synthetic phosphopeptide: CLMKKEFpTLEFSRD (Cys for coupling, plus residues 478 to 490 of human SERCA2a, where pT represents phosphorylated Thr^{484}). Immunization of rabbits using the phosphopeptide was carried out at ChinaPeptides (Shanghai, China), and the site-specific pThr^{484}-SERCA2a antibody was purified on CH-Sepharose coupled to the same peptide.

***In vitro* phosphorylation**

The recombinant GST-SPEG-SK2 and GST-SPEG-SK2^{D3098A} proteins were expressed in *E. coli* and purified using glutathione-Sepharose 4B (GE-Healthcare). The purified GST-SPEG-SK2 wild-type and mutant proteins were used to phosphorylate the Thr^{484} peptide (CLMKKEF**t**LEFSRD, Thr^{484} shown in lower-case bold) *in vitro* at 30°C for 30 min as previously described [32].

Echocardiography (Echo)

Echo was carried out in a double-blinded manner on mice anaesthetized with gaseous isoflurane using a Vevo 770 high-resolution *in vivo* micro-imaging system (VisualSonics, inc) with a 30MHz RMV-707B ultrasonic probe as previously described [33]. M-mode pictures were collected via the ultrasonic probe that was positioned with a 90° angle between the probe and the heart. Left ventricle anterior wall (LVAW), left ventricle posterior wall (LVPW), left ventricle internal dimension (LVID), and left ventricle volume (LV Vol) of systole and diastole were determined on the M-mode tracing in a double-blinded manner and averaged from 6 cardiac cycles. Ejection fraction (EF) is calculated as EF% = [(LV Vol;d - LV Vol;s)/LV Vol;d] x 100%, and fractional shortening (FS) is FS% = [(LVID;d – LVID;s)/LVID;d] x 100%.

Primary cardiomyocyte isolation

Primary mouse cardiomyocytes were isolated using a collagenase-based method and cultured as previously described [34]. Briefly, anaesthetized mice were administered with heparin (5 U per gram of body weight). Mice were terminated 5 min after heparin administration, and the heart was rapidly removed and mounted onto a catheter. Afterwards, the heart was perfused with a collagenase solution (1 mg/ml) using a Langendorff system (ADInstruments). After digestion, the heart tissue was dissociated, and the cell suspension was filtered through a 100 μm cell strainer. The cardiomyocytes were then suspended and precipitated in Krebs-Henseleit buffer B containing 5 mM taurine and 10 mM 2,3-butanedione monoximine with Ca^{2+} (0.1 mM for the first round, 0.2 mM for the second round, and 0.6 mM for the third round). Isolated primary cardiomyocytes were resuspended in Hanks buffer containing 1 mM $MgCl_2$, 1 mM $CaCl_2$ and 2% (w/v) BSA.

Primary neonatal rat cardiomyocytes were isolated and cultured as previously described [35]. Briefly, ventricles of hearts from neonatal rats (postnatal day 0-3) were minced into ~1 mm cubes and digested with 0.25% trypsin at 4°C overnight. On the next day, the trypsin-treated cardiac tissues were further digested with collagenase (1 mg/ml) at 37°C for 15 min, and the resultant cell suspensions were seeded into DMEM containing 10% (v/v) foetal bovine serum for 1 h. Afterwards, fibroblasts were removed, and cardiomyocytes were re-seeded into fresh DMEM plus 10% (v/v) foetal bovine serum. Transfection of plasmids or siRNA was carried out with Lipofectamine 3000 reagent (Thermo Fisher Scientific). The siRNA for rat *Speg* was as follows, 5'-GCUCGAAGCUGGAGAAGAU-3'.

Calcium imaging

Cardiomyocytes were loaded with 5 μM Fluo-4-AM (Thermo Fisher Scientific) and imaged using a Zeiss LSM510 confocal microscope. For calcium sparks, calcium-loaded cells were directly imaged using the confocal microscope. For calcium transient assay in primary mouse cardiomyocytes, calcium-loaded cells were subjected to field stimulation using a GRASS S48 stimulator (frequency 0.5 Hz, duration 60 ms, decay 40 ms, voltage 80V, repeat) when imaged with the confocal microscope. For calcium transient assay in neonatal rat cardiomyocytes, field stimulation was also carried out using a GRASS S48 stimulator (frequency 1 Hz, duration 4 ms, decay 20 ms, voltage 40V,

repeat). For SR calcium load assay, calcium-loaded cells were subjected to field stimulation and then treated with 10 mM caffeine. Line-scan images were taken with the LSM510 confocal microscope and analyzed using IDL5.5 (Harris Geospatial Solutions) as previously described [36]. The decay time (Tau) was measured from the peak of calcium transients to 63% from the peak to the basal level in the fading phase.

Cell culture, transfection and lysis

Human embryonic kidney HEK293 cells were bought from the Cell Resource Center, Chinese Academy of Medical Sciences and Peking Union Medical College (China), and were regularly tested for mycoplasma contamination. Cells were cultured in DMEM medium containing 10% (v/v) foetal bovine serum, and transfected with plasmid DNA using Lipofectamine 3000 reagent (Thermo Fisher Scientific). Two days after transfection, cells were lysed as previously described [30].

Calcium transient assay in HEK293 cells

HEK293 cells were transfected to express SERCA2a together with SPEG or an empty vector, and further cultured for 2 days. After incubated with 5 μM Fluo-4-AM, cells were imaged using an Olympus confocal microscope in a frame scan mode for ~30 sec. Cells were then stimulated with 200 μM carbamylcholine or 100 μM ATP, and images were continuously taken for ~270 sec.

Microsome isolation and Ca^{2+}-ATPase activity assay

Microsomes containing crude ER membrane vesicles were isolated as previously described [37, 38]. The ATPase activity of SERCA2 was determined via measurement of inorganic phosphate (Pi) resulted from ATP hydrolysis as previously described [38]. Briefly, isolated microsomes (50 μg protein) were incubated with an assay buffer containing 100 mM KCl, 10 mM HEPES (pH 7.4), 5 mM $MgCl_2$, 100 μM $CaCl_2$, 1.5 mM ATP, 2 μM A23187 and 5 mM sodium azide in the absence (total activity) or presence of 5 μM thapsigargin (activity of thapsigargin-insensitive calcium pumps) at 30°C for 30 minutes. The reaction was stopped by addition of ice-cold 10% TCA. The amounts of Pi were determined using a colorimetric method [39]. The thapsigargin-sensitive Ca^{2+}-ATPase (SERCA2-ATPase) was calculated by subtraction of thapsigargin-insensitive Ca^{2+}-ATPase activity from total activity.

Ca^{2+} uptake measurement

Ca^{2+} uptake was measured using a Fura-2 based method as previously described [40]. Briefly, microsomes were incubated in assay buffer (100 mM KCl, 10 mM HEPES-KOH (pH 7.4), 10 mM oxalate, 5 mM $MgCl_2$, 10 μM ruthenium red and 2 μM Fura-2 free acid). The uptake reaction was initiated by addition of 5 mM ATP and 2 μM Ca^{2+}. The fluorescence ratio (excitation at 340 and 380 nM) was recorded at 510 nM emission using a fluorescence microplate reader (BioTek). The rate of Ca^{2+} uptake into microsomes was calculated by measuring the linear portion of the slope after addition of Ca^{2+} as previously described [41].

Histology

After termination of mice, hearts were fixed in 4% PFA overnight at 4°C, and histology was carried out as previously described [33]. Hearts were embedded in paraffin wax and sectioned into 5-μm-thick slices using a Leica RM2016 microtome, and heart sections were stained with Hematoxylin-Eosin. Pictures were taken using an Olympus BX53F microscope.

Immunofluorescence staining and imaging

Immunofluorescence staining was carried out as previously described [30]. Heart sections were permeabilized, and sequentially incubated with primary antibodies and fluorophore-conjugated secondary antibodies. Specificity of immunofluorescence staining was verified via using rabbit IgG as a negative control. Pictures were taken with a Leica confocal microscope, and representative images are shown.

Fluorescence resonance energy transfer (FRET) assay

HEK293 cells were transfected with ECFP-SERCA2a and EYFP-SERCA2a plasmids in a 1:1 molar ratio. Two days after transfection, cells were subjected to FRET assays using a Leica SP5 confocal microscope, as described in the Leica FRET Sensitized Emission application manual. Cells co-expressing ECFP-SERCA2a and EYFP-SERCA2a were selected for FRET assay. The FRET efficiency was calculated using the following formula: FRET Efficiency (%) = (FRET signal-β*Donor Signal-γ*Acceptor signal)/(Acceptor signal), where β is obtained with donor only specimen and calculated as $\beta = Signal_{indirectAcceptor}/Signal_{Donor}$, and γ is obtained with acceptor only specimen and calculated as $\gamma = Signal_{IndirectAcceptor}/Signal_{DirectAcceptor}$.

RNA isolation and quantitative PCR (QPCR)

Extraction of total RNA was carried out using the TRIzol® Reagent (Life Technologies), and reverse-transcription was performed using a PrimeScript® RT reagent kit (DRR047A, TaKaRa). QPCR was performed to determine expression levels of target genes using an Applied Biosystems® StepOnePlus™ Real-Time PCR system (Life Technologies). The primers used for QPCR were listed in Online Table I.

Statistical analysis

Data were checked for normal distribution via D'Agostino-Pearson test using Prism software (GraphPad, San Diego, CA, USA). Comparisons were carried out via *t*-test for two groups, or via one-way or two-way ANOVA with Tukey method for post-test for multiple groups as indicated in the figure legends using Prism software (GraphPad, San Diego, CA, USA). Differences were considered statistically significant at $p < 0.05$.

RESULTS

SPEG interacted with SERCA2a and regulated calcium re-uptake into endoplasmic reticulum

We first examined *Speg* expression in mouse models of heart failure induced by isoproterenol or transaortic constriction, and found its mRNA levels were significantly decreased in hearts of both models (Online Figure I A-B). To gain insights how SPEG functions, we overexpressed GFP-SPEG in HEK293 cells and immunoprecipitated it from cell lysates to identify potential interactors for SPEG. Proteins in the immunoprecipitates were identified via mass-spectrometry and subjected to GO term analysis. Proteins possessing calcium-transporting ATPase activity were enriched in the immunoprecipitates, which include SERCA2 (also known as AT2A2), AT2B1, AT2B3 and AT2B4 (Fig. 1A, Online Table II, Online Figure II A). Since SPEG is critical in the heart where SERCA2a plays a key role in regulating calcium homeostasis [3], we then focused on a possible relationship between them. Both proteins localize along the diads where transverse tubules that conduct electrical impulses pair with sarcoplasmic reticular cisternae that mediate Ca^{2+} exchange to control excitation-contraction coupling in cardiomyocytes (Online Figure II B-C). Endogenous SERCA2a could be detected in immunoprecipitates of endogenous SPEG from heart lysates in which proteins were chemically cross-linked with DSP (Fig. 1B). In a reciprocal co-immunoprecipitation experiment,

endogenous SPEG was also found in immunoprecipitates of endogenous SERCA2a from heart lysates (Fig. 1C). Furthermore, GFP-SPEG could interact with HA-SERCA2a when they were co-expressed in HEK293 cells (Fig. 1D). GFP-SPEG did not affect translation and turnover of HA-SERCA2a in HEK293 cells (Online Figure III A-D). Importantly, the full duration at half maximum (FDHM) and time constant Tau of Ca^{2+} transients that are two measures for SERCA2a activity were both significantly decreased while the amplitude of Ca^{2+} transients remained normal when SERCA2a was co-expressed with SPEG in cells as compared with its co-expression with GFP (Fig. 1E-F). These data suggest that expression of SPEG accelerated calcium re-uptake into endoplasmic reticulum via SERCA2a in these cells.

The SK2 of SPEG interacted with SERCA2a and led to its phosphorylation

We next investigated how SPEG regulates SERCA2a. SPEG has two kinase domains, SK1 and SK2, at its C-terminal part (Fig. 2A) [12]. Interaction domain mapping revealed that a fragment $SPEG^{T2946\text{-}end}$ containing SK2 interacted with SERCA2a when co-expressed in cells (Fig. 2B-C). Furthermore, we found that co-expression of SPEG could increase phosphorylation of SERCA2a in HEK293 cells that could be detected with a phospho-Ser/Thr (pSer/Thr) specific antibody (Fig. 2D-E). Asp^{1746} and Asp^{3098} are predicted to be key residues for kinase activities of SK1 and SK2 domains of SPEG, respectively [12]. Interestingly, mutation of Asp^{3098} to alanine abolished the ability of SPEG to phosphorylate SERCA2a while mutation of Asp^{1746} to glycine had no such effect, showing that SK2 of SPEG is responsible for phosphorylation of SERCA2a (Fig. 2F). The FDHM and Tau of Ca^{2+} transients were significantly larger when SERCA2a was co-expressed with $SPEG^{Asp3098Ala}$ than with SPEG wild-type protein (Fig. 2G-H), suggesting that SPEG-mediated phosphorylation of SERCA2a accelerated calcium re-uptake into endoplasmic reticulum. Importantly, expression of SPEG-SK2 in neonatal rat cardiomyocytes significantly decreased the FDHM and Tau of Ca^{2+} transients, and increased their amplitudes (Fig. 2I). In contrast, expression of SPEG-SK1 increased the FDHM and Tau of Ca^{2+} transients in neonatal rat cardiomyocytes, and depressed their amplitudes (Online Figure IV A). In agreement, SPEG-SK1 decreased expression of full-length SPEG in HEK293 cells (Online Figure IV B-C). Therefore, it is likely that expression of SPEG-SK1 delayed Ca^{2+} re-uptake through interference with endogenous SPEG expression. Together, these data show that the SK2 of SPEG interacted with SERCA2a and increased its activity via protein phosphorylation.

As recently reported [15], SPEG could interact with junctophilin-2 (JPH2) when they were co-expressed in cells (Online Figure V A). Interaction domain mapping showed that a fragment $SPEG^{T1563\text{-}S2583}$ containing SK1 but not a fragment $SPEG^{D2584\text{-}end}$ containing SK2 interacted with SERCA2a when co-expressed in cells (Online Figure V B). In contrast to SERCA2a phosphorylation, the $SPEG^{Asp1746Gly}$ mutation but not $SPEG^{Asp3098Ala}$ mutation blunted SPEG-mediated phosphorylation of JPH2 (Online Figure V C). These data demonstrate that the SK1 of SPEG interacted with JPH2 and led to its phosphorylation.

SPEG could promote oligomerization of SERCA2a in a manner dependent on SPEG-mediated phosphorylation

Visualizing blots of SDS-gels revealed that co-expression with SPEG increased the oligomerization of SERCA2a (Fig. 3A), which has been proposed to enhance Ca^{2+}-transporting activity of SERCA2a but not its ATPase activity [8-10]. This effect was further confirmed via a FRET-based assay in which CFP-SERCA2a and YFP-SERCA2a were co-expressed with HA-SPEG

or empty vector (Fig. 3B-C), by the enhanced co-immunoprecipitation of HA-SERCA2a and Flag-SERCA2a from lysates of cells co-transfected with GFP-SPEG as compared to co-transfection with GFP (Fig. 3D).

We then examined whether this SPEG-induced oligomerization of SERCA2a depended on phosphorylation of the latter. Interestingly, the SPEG^{Asp3098Ala} mutant protein failed to increase oligomerization of SERCA2a while mutation of Asp^{1746} to glycine did not affect the ability of SPEG to promote SERCA2a oligomerization in both immunoblotting and FRET assays (Fig. 3E-G), suggesting a dependence of SERCA2a oligomerization on its phosphorylation. We mutated possible phosphorylation sites (www.phosphosite.org) in the cytoplasmic domain of SERCA2a to non-phosphorylatable alanine and assayed its oligomerization status. Through this strategy, Thr^{484} was identified as a key residue for SERCA2a oligomerization (Fig. 3H). A Thr^{484}Ala substitution decreased SPEG-dependent inter-molecular interaction of SERCA2a in all three assays including immunoblotting, FRET and co-immunoprecipitation assays (Fig. 3H-K). Interestingly, the Thr^{484} residue is located in a β-sheet on the nucleotide (N) domain of SERCA2a, and positioned directly beneath a loop region that is involved in the inter-molecular interaction of SERCA2a monomers in a molecular docking model (Online Figure VI A)[10]. SPEG could increase inter-molecular interaction of the N-domain containing cytosolic region of SERCA2a, which was decreased by the Thr^{484}Ala substitution (Online Figure VI B).

Thr^{484} phosphorylation of SERCA2a by SPEG increased its activity

Next, we examined whether SPEG could indeed phosphorylate Thr^{484} of SERCA2a and whether this phosphorylation regulated SERCA2a activity. Eleven phosphorylation sites including pThr^{484} on SERCA2a were also identified through mass-spectrometry when the Ca^{2+} pump was co-expressed with SPEG in HEK293 cells (Fig. 4A). The Thr^{484}Ala mutation prevented SPEG-mediated Ser/Thr phosphorylation of SERCA2a (Online Figure VII A). We raised a site-specific antibody recognizing phosphorylated Thr^{484} on SERCA2a (Online Figure VIII), and further confirmed that co-expression of SPEG could increase Thr^{484} phosphorylation of SERCA2a in HEK293 cells, which was blunted by the Thr^{484}Ala mutation (Fig. 4B). In an *in vitro* phosphorylation assay, the SPEG-SK2 wild-type protein but not the SPEG-SK2^{Asp3098Ala} mutant protein was capable of phosphorylating a Thr^{484} containing peptide (CLMKKEF**t**LEFSRD, Thr^{484} shown in lower-case bold) (Fig. 4C). Thr^{484} phosphorylation of SERCA2a was substantially decreased when *Speg* was knocked down in neonatal rat cardiomyocytes as well as in H9C2 cardiomyocytes (Fig. 4D-E, Online Figure VII B-C). Down-regulation of *Speg* in neonatal rat cardiomyocytes significantly increased the FDHM and Tau of Ca^{2+} transients, and decreased their peaks (Fig. 4F). Importantly, the Thr^{484}Ala substitution augmented the FDHM and Tau of Ca^{2+} transients in HEK293 cells as well as in neonatal rat cardiomyocytes (Fig. 4G, Online Figure VII D-E), and inhibited ER Ca^{2+}-transporting activity in microsomes (Fig. 4H). In contrast, the Thr^{484}Ala substitution did not affect SERCA2a ATPase activity (Fig. 4I). Moreover, expression of SERCA2a^{Thr484Ala} decreased the peaks of Ca^{2+} transients in neonatal rat cardiomyocytes as compared to expression of the wild-type SERCA2a (Fig. 4G). Taken together, these data show that SPEG phosphorylates Thr^{484} of SERCA2a to promote its oligomerization and increase its Ca^{2+}-transporting activity without affecting its ATPase activity.

Cardiac-specific deletion of SPEG decreased Thr^{484} phosphorylation of SERCA2a and caused dilated cardiomyopathy in mice

We next sought to investigate regulation and function of this SPEG−SERCA2a signal nexus *in vivo*. SPEG protein did not change in the heart from E18.5 to postnatal Day-4, but increased from postnatal Day-4 to Day-7 (Online Figure IX A). We mated a *Speg*$^{f/f}$ mouse with an αMHC-Cre mouse [17] to specifically delete *Speg* in the heart after birth. SPEG protein levels were normal in neonates of the *Speg*$^{f/f}$/αMHC-Cre mice (1-day-old) and decreased to ~10% of control levels in the heart but not in skeletal muscle at age of 1 month (Fig. 5A, Online Figure IX B). Importantly, SERCA2a expression was not altered while its Thr^{484} phosphorylation was substantially decreased in the heart of 1-month-old *Speg*$^{f/f}$/αMHC-Cre mice (Fig. 5B), suggesting that SPEG could phosphorylate SERCA2a *in vivo*. The *Speg*$^{f/f}$/αMHC-Cre mice had enlarged hearts with dilation phenotype, and their heart-to-body weight ratios were increased from one month after birth (Fig. 5C, Online Figure IX C-D). Heart function was impaired in the *Speg*$^{f/f}$/αMHC-Cre mice as early as 2-week-old as evidenced by lower ejection fraction and fraction shortening (Fig. 5D-E, Online Figure IX E-F). Substantial cardiac remodeling occurred in the heart of *Speg*$^{f/f}$/αMHC-Cre mice (2-month-old) (Online Figure IX G). As a consequence of dilated cardiomyopathy, the *Speg*$^{f/f}$/αMHC-Cre mice died within 5 months after birth (Online Figure IX H). Since the αMHC-Cre starts to express in the heart from postnatal day 2 when cardiomyocytes still undergo proliferation and maturation [18], it is possible that deletion of *Speg* using the αMHC-Cre still interferes with development of cardiomyocytes, which might contribute to the early death within the first few weeks after birth.

Heart failure can interfere with calcium homeostasis in cardiomyocytes [19]. Cardiac dysfunction occurred in the *Speg*$^{f/f}$/αMHC-Cre mice as early as 2-week-old, which did not allow us to study calcium re-uptake in cardiomyocytes from these knockout mice when their cardiac function was normal. To find such a time window, we mated a *Speg*$^{f/f}$ mouse with a Myh6-MerCreMer (Myh6-MCM) mouse [20] to enable inducible deletion of *Speg* in the adult heart. Before tamoxifen induction, the resultant *Speg*$^{f/f}$/Myh6-MCM mice displayed no overt phenotype and had normal SPEG expression in the heart. After tamoxifen treatment, the levels of SPEG protein in the heart of *Speg*$^{f/f}$/Myh6-MCM mice gradually diminished until less than 10% of control levels could be detected by 4 weeks post tamoxifen induction (Fig. 6A). In contrast, tamoxifen did not affect SPEG expression in skeletal muscle (Online Figure X A). The heart of *Speg*$^{f/f}$/Myh6-MCM mice displayed normal gross morphology by 4 weeks post tamoxifen induction but became dilated with increased ratios of heart to body weight by 8 weeks after tamoxifen treatment (Fig. 6B, Online Figure X B). Importantly, both ejection fraction and fractional shortening remained normal in the *Speg*$^{f/f}$/Myh6-MCM mice until 4 weeks post-tamoxifen induction while these parameters started to decrease 6 weeks after tamoxifen treatment (Fig. 6C-D, Online Figure X L-M). Moreover, the LV volume only started to become enlarged and LV walls thinned in the *Speg*$^{f/f}$/Myh6-MCM mice 6 weeks after induction (Online Figure X C-J). At the molecular level, the *Speg*$^{f/f}$/Myh6-MCM hearts did not undergo significant remodeling 4 weeks after tamoxifen treatment, but they displayed remodeling signatures including up-regulation of cell proliferation, apoptosis, cardiac fibrosis and fetal gene expression from 8 to 12 weeks after induction (Online Figure XI A-G). Masson's trichrome staining also revealed cardiac fibrosis in the *Speg*$^{f/f}$/Myh6-MCM hearts 15 weeks after induction (Online Figure XI H). As a consequence of impaired heart functions, the *Speg*$^{f/f}$/Myh6-MCM mice died within ~24 weeks after tamoxifen induction (Online Figure X K). Since there was no overt change in cardiac function in the *Speg*$^{f/f}$/Myh6-MCM mice at 4 weeks after tamoxifen administration, we chose mice of this stage to

examine impacts of SPEG deficiency on SERCA2a phosphorylation. SERCA2a expression, and expression and phosphorylation of the SERCA2a regulator phospholamban, were all normal in the heart of the *Speg*$^{f/f}$/Myh6-MCM mice at 4 weeks after tamoxifen administration (Online Figure XII A-E). Importantly, Thr^{484} phosphorylation and oligomerization of SERCA2a were both significantly decreased in the heart of the *Speg*$^{f/f}$/Myh6-MCM mice at 4 weeks after tamoxifen induction (Fig. 7A-D). Together, these data demonstrate that SPEG could phosphorylate SERCA2a *in vivo*.

Calcium re-uptake into the SR was delayed in SPEG knockout cardiomyocytes

We next investigated how the disruption of this SPEG-SERCA2a signal nexus affected calcium homeostasis in the heart and primary cardiomyocytes. Rcan1.4 is a target of the Calcineurin-NAFT pathway, and its expression is positively correlated with cytosolic Ca^{2+} [21]. Over-expression of SERCA2a wild-type but not SERCA2a^{T484A} mutant protein in HEK293 cells decreased expression of Rcan1.4 (Online Figure VII F). Interestingly, Rcan1.4 expression started to increase in the *Speg*$^{f/f}$/Myh6-MCM hearts from 4 weeks after induction (Fig. 7E), suggesting that cytosolic Ca^{2+} might become elevated. In agreement, the Ca^{2+}-transporting activity of SERCA2a was significantly decreased, while its ATPase activity remained normal, in microsomes from the *Speg*$^{f/f}$/Myh6-MCM hearts at 4 weeks after induction (Fig. 7F). To gain further insights, we isolated primary cardiomyocytes from the *Speg*$^{f/f}$ and *Speg*$^{f/f}$/Myh6-MCM mice at 4, 6 and 8 weeks after tamoxifen administration and examined their calcium homeostasis. The sizes of primary cardiomyocytes were comparable between the two genotypes at 4 weeks after induction (Online Figure XIII A-C). Electrical stimulation triggered calcium transients with comparable amplitudes in the two genotypes of primary cardiomyocytes at 4 weeks after induction (Fig. 8A-B). In contrast, the FDHM and Tau were both significantly increased in the SPEG knockout cardiomyocytes at 4 weeks after induction (Fig. 8A-B), suggesting that calcium re-uptake into the SR through SERCA2a was delayed in these cells. At 6 and 8 weeks after induction, Ca^{2+}-transients were significantly depressed in SPEG knockout cardiomyocytes (Fig. 8C, Online Figure XIV A). Again, the FDHM and Tau were both significantly augmented in the SPEG knockout cardiomyocytes (Fig. 8C, Online Figure XIV A). Caffeine treatment revealed that the SR calcium load remained normal in SPEG deficient cardiomyocytes at 4 weeks after induction, but it became significantly lower in SPEG knockout cardiomyocytes than in control cells at 6 weeks after induction (Fig. 8D). The decay time of the caffeine-induced Ca^{2+} peak was normal in SPEG knockout cardiomyocytes (Fig. 8D), suggesting that the activity of Na^{+}/Ca^{2+} exchanger (NCX) was not altered. The late onsets of depressed amplitude of Ca^{2+}-transients and decreased SR Ca^{2+} load suggest that these changes might be secondary to impaired SR Ca^{2+} re-uptake. This may also help to explain why co-expression of SPEG and SERCA2a in HEK293 cells decreased the Tau of Ca^{2+}-transients but had no effect on Ca^{2+}-amplitude. Co-expression of SPEG and SERCA2a in HEK293 cells probably did not last long enough to produce a detectable change in Ca^{2+}-amplitude using our detection method. We further determined spontaneous SR Ca^{2+} release and found that frequency of Ca^{2+} sparks was unaltered in SPEG deficient cardiomyocytes at all the three time points (Fig. 8E-F, Online Figure XIV B), suggesting that Ca^{2+} release from the SR through ryanodine receptor 2 (RyR2) was normal. The amplitude of Ca^{2+} sparks was normal at 4 weeks but displayed a small decrease at 6 weeks in SPEG knockout cardiomyocytes (Fig. 8E-F). Importantly, both FDHM and tau of Ca^{2+} sparks were significantly increased in SPEG deficient cardiomyocytes at all the three time points (Fig. 8E-F, Online Figure XIV B), further

suggesting that SERCA2a activity was decreased. Together, these data demonstrate that SPEG regulates Ca^{2+} re-uptake into the SR through SERCA2a, and that impaired Ca^{2+} re-uptake preceded cardiac dysfunction and dilation in the heart of the *Speg*$^{f/f}$/Myh6-MCM mice after tamoxifen treatment.

DISCUSSIONS

In this study, we identified SPEG as an important regulator for SERCA2a in the heart and demonstrated that SPEG regulated calcium re-uptake into the SR through phosphorylating SERCA2a by its SK2 in cardiomyocytes.

SPEG is a poorly-studied protein kinase although it has recently been recognized as an important player in regulating cardiac development and function [13]. It belongs to the MLCK subgroup of CaMK Ser/Thr protein kinase family and has two kinase domains in its C-terminal region [12]. The SK1 of SPEG displays more similarity with other kinase members within the MLCK group than does the SK2 [12]. Moreover, our data demonstrate that the SK2 of SPEG is responsible for phosphorylation of Thr^{484} on SERCA2a, while the SK1 but not the SK2 can phosphorylate JPH2. These results suggest that the SK1 and SK2 of SPEG play distinct roles in the heart. How these two kinase domains fulfil such functional diversity remains unclear. One possibility is that the SK1 and SK2 of SPEG have different sequence preferences for their substrate phosphorylation. Identification of the SK1-mediated phosphorylation site(s) on JPH2 may help to determine the sequence preferences for these two kinase domains in the future. Another possibility is that the SK1 and SK2 of SPEG may have distinct abilities to interact with their substrates, and thereby phosphorylate different proteins. In line with this possibility, the two kinase-domains displayed different capacities to interact with their respective substrates JPH2 and SERCA2a. Previous studies mainly focused on the physiological function of SPEG, and little is known about its regulation [12, 13, 15]. Interestingly, SPEG has a putative calmodulin binding site between SK1 and SK2 [22], suggesting its potential regulation by calcium. Given the role of SPEG-SK2 in control of SERCA2a, potential binding of calmodulin to SPEG suggests a possible feedback loop to regulate SPEG activity. The loss of whole SPEG protein not only affects SK2-SERCA2a dependent Ca^{2+} re-uptake, but also impairs downstream events dependent on SK1 or other domains of SPEG, which might be intertwined to cause the death of *Speg*$^{f/f}$/Myh6-MCM mice after tamoxifen induction. Certainly, more work needs to be done in order to understand how these two kinase domains function and how they are regulated.

Restoration of SERCA2a expression and/or activity is an attractive strategy to treat heart failure [3]. SERCA2a is subjected to multiple post-translational modifications including SUMOylation [4], nitration [5] and glutathiolation [6]. Experimental medicines targeting SUMOylation of SERCA2a through gene transfer of SUMO-1 or small molecule activator have been shown to improve cardiac function in the failing heart [23, 24]. Interestingly, the Thr^{484} residue identified to regulate oligomerization of SERCA2a is close to one of the SUMOylation sites Lys^{480} that is critical for preserving SERCA2a activity and stability [4]. Whether, and how, phosphorylation of Thr^{484} interacts with SUMOylation of Lys^{480} to regulate SERCA2a is an intriguing open question. The dimer model of SERCA2a via molecular docking reveals inter-molecular interaction primarily through residues in its N-domain that can undergo conformational changes and/or domain motions to promote interaction of SERCA2a monomers [10]. Since Thr^{484} is positioned directly beneath a loop region that is involved in inter-molecular interaction of SERCA2a in this molecular docking model, we suspect that Thr^{484}

phosphorylation by SPEG might cause conformational changes and/or motions of the N-domain, which then promotes oligomerization of SERCA2a. Lys^{480} is located on the same β-sheet of the N-domain as Thr^{484}, which raises a further question about whether SUMOylation of SERCA2a also regulates its oligomerization. Previous studies have shown that the ATPase activity of SERCA does not depend on inter-molecular interaction between SERCA monomers [25, 26]. However, the ATPase activity is coupled with Ca^{2+}-transport within the oligomer of SERCA, and Ca^{2+} transport is strongly correlated with the inter-molecular interaction of functional SERCA monomers [11, 27]. Our findings further demonstrate the importance of Thr^{484} phosphorylation dependent SERCA2a oligomerization in controlling Ca^{2+}-transport, which open new possibilities to modulate SERCA2a activity.

When SERCA2 was deleted in mouse heart using the tamoxifen-inducible Cre, the Tau of Ca^{2+}-transient was increased by ~90-118% in SERCA2-deficient cardiomyocytes [28, 29]. Impaired SR Ca^{2+} re-uptake preceded functional alterations of the SERCA2-deficient heart detected via echocardiography [28]. The Tau of Ca^{2+}-transient was augmented by ~40% in SPEG-deficient cardiomyocytes in which SERCA2a-Thr^{484} phosphorylation was markedly decreased. Furthermore, our data demonstrate that impaired SERCA2a Thr^{484} phosphorylation and delayed Ca^{2+} re-uptake into the SR also occurred before morphological and functional alterations of the heart of *Speg*$^{f/f}$/Myh6-MCM mice, which is at least one of the causes for heart failure in these mice. The different onsets of impaired SR Ca^{2+} re-uptake and cardiac dysfunction in echocardiographic assessment might reflect the causal relationship between these two events in these mouse models. Alternatively, the two assays might have different sensitivities. Echocardiographic assessment is carried out at the organ level, and might not be sensitive enough to detect subtle changes in cardiac function, if there is any, in the SERCA2 knockout mice or our *Speg*$^{f/f}$/Myh6-MCM mice at 4 weeks after tamoxifen induction.

Quick et al recently reported generation of *Speg*$^{f/f}$/Myh6-MCM mice using the same ES cells [15]. In that case, the *Speg*$^{f/f}$/Myh6-MCM mice started to die as early as 2 weeks after administration with tamoxifen (dosage unspecified in [15]) and nearly half of the mice died at 4 weeks post tamoxifen administration. In our case, the *Speg*$^{f/f}$/Myh6-MCM mice displayed no morphological or functional alterations in their heart at 4 weeks post administration with tamoxifen (20 mg/kg/d for five consecutive days) and started to die at 13 weeks post tamoxifen administration. We do not know exactly why the onset and progression of cardiac dysfunction differ in these two cases although we suspect that it might be due to different dosage of tamoxifen used for induction. Nevertheless, different dosage of tamoxifen and kinetics of disease progression together with other experimental conditions might impact on the measurements on calcium re-uptake in cardiomyocytes, which differed between the two studies. Both studies demonstrate that SR Ca^{2+} release through RyR2 was normal in SPEG-deficient cardiomyocytes before heart failure. Quick et al also showed that SR Ca^{2+} release was decreased in SPEG-deficient cardiomyocytes at 8 weeks after administration with tamoxifen when the hearts were failing, which was proposed to be secondary in these failing hearts [15]. Our time course studies of Ca^{2+} homeostasis in cardiomyocytes consistently revealed delays in SR Ca^{2+} re-uptake at 4, 6 and 8 weeks after tamoxifen induction, which might lead to a decrease of SR Ca^{2+} load and an elevation of Ca^{2+} in the cytoplasm. Despite these differences, these two studies demonstrate the importance of SPEG in maintaining heart function in adulthood, whose down-regulation is associated with cardiac dysfunction in certain diseases.

In summary, we show that the SK1 and SK2 of SPEG may play distinct roles in the heart. The SK2 of SPEG regulates calcium re-uptake into the SR through interaction and phosphorylation of SERCA2a in cardiomyocytes. SPEG may serve as a new target to modulate SERCA2a activation for treatment of heart diseases with impaired calcium homeostasis.

Author contributions

C.Q., M.L., Q.D., Q.L.C., H.W., D.C., L.F., B.X., K.F.O.Y. performed experiments, analyzed data and reviewed the manuscript. X.G. reviewed the manuscript. C.M. reviewed and edited the manuscript. H.Y.W. and S.C. designed experiments, analyzed data, and wrote the manuscript. S.C. is the guarantor of this study. All authors approved the final version of the manuscript.

Competing financial interests

The authors declare no competing financial interests.

Acknowledgements

We thank members at the Animal Resource Unit, Liver Disease Collaborative Research Platform of Medical School, and Translational Medicine Core Facilities of Medical School of Nanjing University for technical assistance. We thank Dr. Shiqiang Wang (Peking University, China) for providing the rat JPH2 cDNA. Thanks to the Ministry of Science and Technology of China (Grant Nos. 2014CB964704 (the National Basic Research Program of China) and 2014BAI02B01 (the National Science and Technology Support Project)), the National Natural Science Foundation of China (Grant Nos. 31671456 and 31571211), the Ministry of Education of China (Grant Nos. 20120091120048 and NCET-13-0270), and the Science and Technology Foundation of Jiangsu Province of China (Grant No. BK20161393 (Basic Research Program)), for financial support.

References

1. Braunwald E. The war against heart failure: The lancet lecture. *Lancet*. 2015;385:812-824
2. Gorski PA, Ceholski DK, Hajjar RJ. Altered myocardial calcium cycling and energetics in heart failure--a rational approach for disease treatment. *Cell Metab*. 2015;21:183-194
3. Kho C, Lee A, Hajjar RJ. Altered sarcoplasmic reticulum calcium cycling--targets for heart failure therapy. *Nat Rev Cardiol*. 2012;9:717-733
4. Kho C, Lee A, Jeong D, Oh JG, Chaanine AH, Kizana E, Park WJ, Hajjar RJ. Sumo1-dependent modulation of serca2a in heart failure. *Nature*. 2011;477:601-605
5. Knyushko TV, Sharov VS, Williams TD, Schoneich C, Bigelow DJ. 3-nitrotyrosine modification of serca2a in the aging heart: A distinct signature of the cellular redox environment. *Biochemistry*. 2005;44:13071-13081
6. Adachi T, Weisbrod RM, Pimentel DR, Ying J, Sharov VS, Schoneich C, Cohen RA. S-glutathiolation by peroxynitrite activates serca during arterial relaxation by nitric oxide. *Nat Med*. 2004;10:1200-1207
7. Toyofuku T, Curotto Kurzydlowski K, Narayanan N, MacLennan DH. Identification of ser38 as the site in cardiac sarcoplasmic reticulum ca(2+)-atpase that is phosphorylated by ca2+/calmodulin-dependent protein kinase. *J Biol Chem*. 1994;269:26492-26496
8. Lennon NJ, Harmon S, Mackey A, Ohlendieck K. Oligomerization of the sarcoplasmic reticulum ca2+-atpase serca2 in cardiac muscle. *Mol Cell Biol Res Commun*. 1999;1:182-187
9. Blackwell DJ, Zak TJ, Robia SL. Cardiac calcium atpase dimerization measured by cross-linking and fluorescence energy transfer. *Biophys J*. 2016;111:1192-1202

10. Chen LT, Yao Q, Soares TA, Squier TC, Bigelow DJ. Phospholamban modulates the functional coupling between nucleotide domains in ca-atpase oligomeric complexes in cardiac sarcoplasmic reticulum. *Biochemistry*. 2009;48:2411-2421
11. Ushimaru M, Fukushima Y. The dimeric form of ca2+-atpase is involved in ca2+ transport in the sarcoplasmic reticulum. *Biochem J*. 2008;414:357-361
12. Hsieh CM, Fukumoto S, Layne MD, Maemura K, Charles H, Patel A, Perrella MA, Lee ME. Striated muscle preferentially expressed genes alpha and beta are two serine/threonine protein kinases derived from the same gene as the aortic preferentially expressed gene-1. *J Biol Chem*. 2000;275:36966-36973
13. Liu X, Ramjiganesh T, Chen YH, Chung SW, Hall SR, Schissel SL, Padera RF, Jr., Liao R, Ackerman KG, Kajstura J, Leri A, Anversa P, Yet SF, Layne MD, Perrella MA. Disruption of striated preferentially expressed gene locus leads to dilated cardiomyopathy in mice. *Circulation*. 2009;119:261-268
14. Liu X, Hall SR, Wang Z, Huang H, Ghanta S, Di Sante M, Leri A, Anversa P, Perrella MA. Rescue of neonatal cardiac dysfunction in mice by administration of cardiac progenitor cells in utero. *Nat Commun*. 2015;6:8825
15. Quick AP, Wang Q, Philippen LE, Barreto-Torres G, Chiang DY, Beavers D, Wang G, Khalid M, Reynolds JO, Campbell HM, Showell J, McCauley MD, Scholten A, Wehrens XH. Speg (striated muscle preferentially expressed protein kinase) is essential for cardiac function by regulating junctional membrane complex activity. *Circ Res*. 2017;120:110-119
16. Agrawal PB, Pierson CR, Joshi M, Liu X, Ravenscroft G, Moghadaszadeh B, Talabere T, Viola M, Swanson LC, Haliloglu G, Talim B, Yau KS, Allcock RJ, Laing NG, Perrella MA, Beggs AH. Speg interacts with myotubularin, and its deficiency causes centronuclear myopathy with dilated cardiomyopathy. *Am J Hum Genet*. 2014;95:218-226
17. Agah R, Frenkel PA, French BA, Michael LH, Overbeek PA, Schneider MD. Gene recombination in postmitotic cells. Targeted expression of cre recombinase provokes cardiac-restricted, site-specific rearrangement in adult ventricular muscle in vivo. *J Clin Invest*. 1997;100:169-179
18. Davis J, Maillet M, Miano JM, Molkentin JD. Lost in transgenesis: A user's guide for genetically manipulating the mouse in cardiac research. *Circ Res*. 2012;111:761-777
19. Beuckelmann DJ, Nabauer M, Erdmann E. Intracellular calcium handling in isolated ventricular myocytes from patients with terminal heart failure. *Circulation*. 1992;85:1046-1055
20. Sohal DS, Nghiem M, Crackower MA, Witt SA, Kimball TR, Tymitz KM, Penninger JM, Molkentin JD. Temporally regulated and tissue-specific gene manipulations in the adult and embryonic heart using a tamoxifen-inducible cre protein. *Circ Res*. 2001;89:20-25
21. Yang J, Rothermel B, Vega RB, Frey N, McKinsey TA, Olson EN, Bassel-Duby R, Williams RS. Independent signals control expression of the calcineurin inhibitory proteins mcip1 and mcip2 in striated muscles. *Circ Res*. 2000;87:E61-68
22. Gautel M. Cytoskeletal protein kinases: Titin and its relations in mechanosensing. *Pflugers Arch*. 2011;462:119-134

23. Tilemann L, Lee A, Ishikawa K, Aguero J, Rapti K, Santos-Gallego C, Kohlbrenner E, Fish KM, Kho C, Hajjar RJ. Sumo-1 gene transfer improves cardiac function in a large-animal model of heart failure. *Sci Transl Med*. 2013;5:211ra159
24. Kho C, Lee A, Jeong D, Oh JG, Gorski PA, Fish K, Sanchez R, DeVita RJ, Christensen G, Dahl R, Hajjar RJ. Small-molecule activation of serca2a sumoylation for the treatment of heart failure. *Nat Commun*. 2015;6:7229
25. Andersen JP, Moller JV, Jorgensen PL. The functional unit of sarcoplasmic reticulum ca2+-atpase. Active site titration and fluorescence measurements. *J Biol Chem*. 1982;257:8300-8307
26. Moller JV, Lind KE, Andersen JP. Enzyme kinetics and substrate stabilization of detergent-solubilized and membraneous (ca2+ + mg2+)-activated atpase from sarcoplasmic reticulum. Effect of protein-protein interactions. *J Biol Chem*. 1980;255:1912-1920
27. Nagata Y, Nakamura J, Yamamoto T. Temperature sensitivity of proteoliposomes reconstituted from a mixture of scallop and rabbit sarcoplasmic reticulum ca2+-atpases. *J Biochem*. 1997;121:648-653
28. Andersson KB, Birkeland JA, Finsen AV, Louch WE, Sjaastad I, Wang Y, Chen J, Molkentin JD, Chien KR, Sejersted OM, Christensen G. Moderate heart dysfunction in mice with inducible cardiomyocyte-specific excision of the serca2 gene. *J Mol Cell Cardiol*. 2009;47:180-187
29. Li L, Louch WE, Niederer SA, Aronsen JM, Christensen G, Sejersted OM, Smith NP. Sodium accumulation in serca knockout-induced heart failure. *Biophys J*. 2012;102:2039-2048
30. Chen L, Chen Q, Xie B, Quan C, Sheng Y, Zhu S, Rong P, Zhou S, Sakamoto K, MacKintosh C, Wang HY, Chen S. Disruption of the ampk-tbc1d1 nexus increases lipogenic gene expression and causes obesity in mice via promoting igf1 secretion. *Proc Natl Acad Sci U S A*. 2016;113:7219-7224
31. Dubois F, Vandermoere F, Gernez A, Murphy J, Toth R, Chen S, Geraghty KM, Morrice NA, MacKintosh C. Differential 14-3-3 affinity capture reveals new downstream targets of phosphatidylinositol 3-kinase signaling. *Mol Cell Proteomics*. 2009;8:2487-2499
32. Chen Q, Quan C, Xie B, Chen L, Zhou S, Toth R, Campbell DG, Lu S, Shirakawa R, Horiuchi H, Li C, Yang Z, MacKintosh C, Wang HY, Chen S. Garnl1, a major ralgap alpha subunit in skeletal muscle, regulates insulin-stimulated rala activation and glut4 trafficking via interaction with 14-3-3 proteins. *Cell Signal*. 2014;26:1636-1648
33. Quan C, Xie B, Wang HY, Chen S. Pkb-mediated thr649 phosphorylation of as160/tbc1d4 regulates the r-wave amplitude in the heart. *PLoS One*. 2015;10:e0124491
34. Xu X, Yang D, Ding JH, Wang W, Chu PH, Dalton ND, Wang HY, Bermingham JR, Jr., Ye Z, Liu F, Rosenfeld MG, Manley JL, Ross J, Jr., Chen J, Xiao RP, Cheng H, Fu XD. Asf/sf2-regulated camkiidelta alternative splicing temporally reprograms excitation-contraction coupling in cardiac muscle. *Cell*. 2005;120:59-72
35. Dittami GM, Rajguru SM, Lasher RA, Hitchcock RW, Rabbitt RD. Intracellular calcium transients evoked by pulsed infrared radiation in neonatal cardiomyocytes. *J Physiol*. 2011;589:1295-1306

36. Ouyang K, Wu C, Cheng H. Ca(2+)-induced ca(2+) release in sensory neurons: Low gain amplification confers intrinsic stability. *J Biol Chem*. 2005;280:15898-15902
37. Parsons JT, Churn SB, Kochan LD, DeLorenzo RJ. Pilocarpine-induced status epilepticus causes n-methyl-d-aspartate receptor-dependent inhibition of microsomal mg(2+)/ca(2+) atpase-mediated ca(2+) uptake. *J Neurochem*. 2000;75:1209-1218
38. Wang Y, Bruce AT, Tu C, Ma K, Zeng L, Zheng P, Liu Y, Liu Y. Protein aggregation of serca2 mutants associated with darier disease elicits er stress and apoptosis in keratinocytes. *J Cell Sci*. 2011;124:3568-3580
39. Ames BN. Assay of inorganic phosphate, total phosphate and phosphatases. *Methods in Enzymology*. 1966;8:115-118
40. Kargacin ME, Kargacin GJ. Methods for determining cardiac sarcoplasmic reticulum ca2+ pump kinetics from fura 2 measurements. *Am J Physiol*. 1994;267:C1145-1151
41. Pelled D, Lloyd-Evans E, Riebeling C, Jeyakumar M, Platt FM, Futerman AH. Inhibition of calcium uptake via the sarco/endoplasmic reticulum ca2+-atpase in a mouse model of sandhoff disease and prevention by treatment with n-butyldeoxynojirimycin. *J Biol Chem*. 2003;278:29496-29501

Figure Legends

Figure 1 Identification of SERCA2a as a SPEG-interacting protein

A. GFP-SPEG fusion protein was expressed in HEK293 cells and immunoprecipitated from cell lysates using the GFP-binder. Mock immunoprecipitation was performed using HEK293 cell lysates. The protein bands shown in brackets were excised, digested with trypsin and identified via mass-spectrometry.

B. Endogenous SPEG was immunoprecipitated from heart lysates that were cross-linked using a cross-linker DSP, and endogenous SERCA2a was detected in the immunoprecipitates using the goat anti-SERCA2a antibody.

C. Endogenous SERCA2a was immunoprecipitated using the mouse anti-SERCA2a antibody from heart lysates that were cross-linked using a cross-linker DSP, and endogenous SPEG was detected in the immunoprecipitates.

D. Flag-SERCA2a was co-expressed with GFP-SPEG or free GFP in HEK293 cells. Co-immunoprecipitated Flag-SERCA2a was detected in the immunoprecipitates of GFP-SPEG or free GFP via western blot.

E-F. Calcium transients in HEK293 cells expressing mCherry-SERCA2a together with HA-SPEG or empty vector. Calcium transients were recorded using a confocal microscopy in cells that were stimulated with carbamylcholine. Full duration at half maximum (FDHM) (E) and time constant Tau (F) of calcium transients were quantified. n = 86-89.

The data are given as the mean ± SEM. *** indicates $p < 0.001$.

Figure 2 Regulation of SERCA2a and calcium re-uptake by the SK2 of SPEG

A. Diagrammatic illustration of domain composition of SPEG. SK, serine/threonine (Ser/Thr) kinase domain. CBD, calmodulin-binding domain. Asp^{1746} and Asp^{3098} are predicted to be key residues for kinase activities of SK1 and SK2 domains of SPEG, respectively

B-C. GFP-tagged SPEG fragments were co-expressed with HA-SERCA2a in HEK293 cells. GFP-tagged SPEG fragments were immunoprecipitated from cell lysates using the GFP-binder, and HA-SERCA2a was detected in the immunoprecipitates using the HA antibody via western blot.

D-E. Phosphorylation of SERCA2a by SPEG. HA-SERCA2a was co-expressed with GFP-SPEG or free GFP in HEK293 cells, and immunoprecipitated from cell lysates using an HA antibody. Phosphorylation of SERCA2a was detected on the immunoprecipitated HA-SERCA2a using an antibody recognizing phosphorylated serine/threonine residues (pSer/Thr). E shows quantitation of phosphorylation of HA-SERCA2a using the blot shown in D.

F. Flag-SERCA2a was co-expressed with GFP-SPEG WT or mutant proteins in HEK293 cells. After immunoprecipitated from cell lysates, phosphorylation of Flag-SERCA2a was detected using the pSer/Thr antibody.

G-H. Calcium transients in HEK293 cells expressing mCherry-SERCA2a together with HA-SPEG or HA-$SPEG^{D3098A}$ mutant protein. Calcium transients were recorded using a confocal microscopy in cells that were stimulated with ATP. G, curves of calcium transients. H, quantitation of full duration at half maximum (FDHM) and time constant Tau of calcium transients. n = 61-68.

I. Calcium transients in neonatal rat cardiomyocytes expressing mCherry-SPEG-SK2 or mCherry alone (vector) upon field stimulation. Amplitudes, FDHM and Tau of calcium transients were quantified from 24 (vector) or 26 (mCherry-SPEG-SK2) cells.

The data in H are given as the mean ± SEM. The bars in the scatter plots show the mean ± SEM. * indicates $p < 0.05$, ** $p < 0.01$, and *** $p < 0.001$.

Figure 3 Thr^{484} as a key residue for regulation of SERCA2a oligomerization by the SPEG-SK2

A. HA-SERCA2a was co-expressed with GFP-SPEG or free GFP in HEK293 cells. Oligomerization of HA-SERCA2a was determined via western blot.

B-C. FRET assay for measurements of inter-molecular interaction of SERCA2a in the presence of SPEG. Two experimental groups were set up for transfection of HEK293 cells. In the experimental group, CFP-SERCA2a and YFP-SERCA2a were co-expressed with HA-SPEG. In the control group, CFP-SERCA2a and YFP-SERCA2a were co-expressed with an empty vector. B, representative images for FRET. C, quantitative data on FRET efficiency. n = 22-39. Bars indicate 5 μm in length.

D. HA-SERCA2a was co-expressed with Flag-SERCA2a in the presence of GFP-SPEG or free GFP in HEK293 cells. Flag-SERCA2a was immunoprecipitated from cell lysates, and the abundance of HA-SERCA2a in the immunoprecipitates was detected via immunoblotting.

E. Flag-SERCA2a was co-expressed with GFP-SPEG WT or mutant proteins in HEK293 cells. Oligomerization of Flag-SERCA2a was determined via western blot.

F-G. FRET assay for measurements of inter-molecular interaction of SERCA2a in the presence of WT or mutant SPEG. Four experimental groups were set up for transfection of HEK293 cells. In the control group, CFP-SERCA2a and YFP-SERCA2a were co-expressed with an empty vector. In the other three groups, CFP-SERCA2a and YFP-SERCA2a were co-expressed with HA-SPEG WT or mutant proteins. F. Quantitative data on FRET efficiency. n = 23-36. G. Representative images for FRET. Bars indicate 5 μm in length. Statistical analysis was carried out via one-way ANOVA.

H. HA-SERCA2a WT and mutant proteins were co-expressed with GFP-SPEG or free GFP in HEK293 cells. Oligomerization of HA-SERCA2a was determined via western blot.

I-J. FRET assay for measurements of inter-molecular interaction of SERCA2a WT or Thr^{484}Ala mutant proteins in the presence of SPEG. Three experimental groups were set up for transfection of HEK293 cells. In the control group, CFP-SERCA2a and YFP-SERCA2a were co-expressed with an empty vector. In the second group, CFP-SERCA2a and YFP-SERCA2a were co-expressed with HA-SPEG. In the third group, CFP-SERCA2a^{T484A} and YFP-SERCA2a^{T484A} were co-expressed with HA-SPEG. I. Quantitative data on FRET efficiency. n = 29-38. J. Representative images for FRET. Bars indicate 5 μm in length. Statistical analysis was carried out via one-way ANOVA.

K. HA-SERCA2a WT and Thr^{484}Ala mutant proteins were co-expressed with Flag-SERCA2a WT and Thr^{484}Ala mutant proteins in the presence of GFP-SPEG in HEK293 cells. Flag-SERCA2a WT and mutant proteins were immunoprecipitated from cell lysates, and the abundance of HA-SERCA2a WT and mutant proteins in the immunoprecipitates were detected via immunoblotting.

The bars in the scatter plots show the mean ± SEM. * indicates $p < 0.05$, and *** indicates $p < 0.001$. ns, not significant.

Figure 4 Effects of SERCA2a-Thr^{484} phosphorylation by the SPEG-SK2 on its Ca^{2+} transport activity

A. HA-SERCA2a was co-expressed with GFP-SPEG in HEK293 cells. HA-SERCA2a was immunoprecipitated from cell lysates using the HA antibody, excised from the gel, and digested with

trypsin. Phosphorylated peptides of HA-SERCA2a were identified via mass-spectrometry. Phosphorylation sites were highlighted in red.

B. Flag-SERCA2a WT and $Thr^{484}Ala$ mutant proteins were expressed in HEK293 cells together with GFP-SPEG or free GFP. Flag-SERCA2a WT and mutant proteins were immunoprecipitated from cell lysates, and their phosphorylation was detected using the $pThr^{484}$-SERCA2a antibody.

C. *In vitro* phosphorylation of the SERCA2a-Thr^{484} by the recombinant GST-SPEG-SK2 wild-type and GST-SPEG-$SK2^{D3098A}$ mutant proteins. The Thr^{484} peptide (CLMKKEF**t**LEFSRD, Thr^{484} shown in lower-case bold) was used in the *in vitro* phosphorylation assay. The indicated amounts of peptides (15 ng per spot in the upper row and 30 ng per spot in the lower row) were spotted onto nitrocellulose and detected with the $pThr^{484}$-SERCA2a antibody. The $pThr^{484}$ peptide (CLMKKEFpTLEFSRD) was used as a positive control.

D-E. SERCA2a-Thr^{484} phosphorylation in neonatal rat cardiomyocytes upon knockdown of *Speg* via siRNA. D, representative blots and quantitative data for SPEG protein. E, representative blots and quantitative data for SERCA2a-Thr^{484} phosphorylation. n = 12.

F. Calcium transients in *Speg*-depleted neonatal rat cardiomyocytes upon field stimulation. Amplitudes, FDHM and Tau of calcium transients were quantified from 111 (siNC) or 107 (siSpeg) cells.

G. Calcium transients in neonatal rat cardiomyocytes expressing mCherry-SERCA2a WT or mCherry-SERCA2a-Thr^{484} mutant proteins upon field stimulation. Amplitudes, FDHM and Tau of calcium transients were quantified from 52 (mCherry-SERCA2a WT) or 46 (mCherry-SERCA2a-Thr^{484}) cells.

H-I. SERCA2a Ca^{2+}-transporting activity and ATPase activity in microsomes isolated HEK293 cells expressing the indicated proteins. H, SERCA2a Ca^{2+}-transporting activity (n = 10). I, SERCA2a ATPase activity (n = 4). Statistical analysis was carried out via one-way ANOVA.

The data in F-G are given as the mean ± SEM. The bars in the scatter plots show the mean ± SEM. * indicates $p < 0.05$, ** $p < 0.01$, and *** $p < 0.001$.

Figure 5 SERCA2a-Thr^{484} phosphorylation and cardiac function in the *Speg*$^{f/f}$/αMHC-Cre mice

A. Expression of SPEG and SERCA2a in the heart of *Speg*$^{f/f}$ and *Speg*$^{f/f}$/αMHC-Cre mice after birth.

B. Thr^{484} phosphorylation of SERCA2a in the heart of *Speg*$^{f/f}$ and *Speg*$^{f/f}$/αMHC-Cre mice (1-month-old).

C. Cardiac morphology of the *Speg*$^{f/f}$/αMHC-Cre mice and *Speg*$^{f/f}$ littermates (2-month-old). Bars indicate 2 mm in length.

D-E. Echocardiography was performed on the anaesthetized male *Speg*$^{f/f}$/αMHC-Cre mice and *Speg*$^{f/f}$ littermates at the indicated ages to measure ejection fraction (D) and fractional shortening (E). The data are given as the mean ± SEM. Statistical analysis was carried out via two-way ANOVA. n = 6-8. *** indicates $p < 0.001$.

Figure 6 Inducible deletion of SPEG in the *Speg*$^{f/f}$/Myh6-MCM mice

A. SPEG expression in the heart of *Speg*$^{f/f}$ and *Speg*$^{f/f}$/Myh6-MCM mice before and after tamoxifen induction.

B. Cardiac morphology of the male *Speg*$^{f/f}$/Myh6-MCM mice and *Speg*$^{f/f}$ littermates before and after tamoxifen induction.

C-D. Ejection fraction (C) and fractional shortening (D) in the *Speg*$^{f/f}$ and *Speg*$^{f/f}$/Myh6-MCM mice before and after tamoxifen induction. The data are given as the mean ± SEM. Statistical analysis was carried out via two-way ANOVA. n = 12-25. *** indicates $p < 0.001$.

Figure 7 SERCA2a-Thr^{484} phosphorylation and activities in the heart of *Speg*$^{f/f}$/Myh6-MCM mice after tamoxifen induction

A-B. Thr^{484} phosphorylation of SERCA2a in the heart of *Speg*$^{f/f}$ and *Speg*$^{f/f}$/Myh6-MCM mice (4 weeks after tamoxifen induction). B shows quantitation of SERCA2a Thr^{484} phosphorylation using the blot shown in A.

C-D. Oligomerization of SERCA2a in the heart of *Speg*$^{f/f}$ and *Speg*$^{f/f}$/Myh6-MCM mice (4 weeks after tamoxifen induction). D shows quantitation of SERCA2a oligomerization (ratio of oligomer to monomer) using the blot shown in C.

E. Rcan1.4 expression in the heart of *Speg*$^{f/f}$ and *Speg*$^{f/f}$/Myh6-MCM mice at the indicated time before and after tamoxifen induction. n = 4-6.

F. SERCA2a Ca^{2+}-transporting activity (n = 15) and ATPase activity (n=5) in microsomes isolated from the heart of *Speg*$^{f/f}$ and *Speg*$^{f/f}$/Myh6-MCM mice (4 weeks after tamoxifen induction).

The bars in the scatter plots show the mean ± SEM. * indicates $p < 0.05$, and ** $p < 0.01$.

Figure 8 Ca^{2+} homeostasis in primary cardiomyocytes from the the *Speg*$^{f/f}$/Myh6-MCM mice after tamoxifen induction

A-B. Calcium transients elicited by electrical stimulation in primary cardiomyocytes isolated from the *Speg*$^{f/f}$ and *Speg*$^{f/f}$/Myh6-MCM mice at 4 weeks after tamoxifen induction. A. Representative calcium transient images and curves. B. Quantitation of amplitudes, full duration at half maximum (FDHM) and time constant Tau of calcium transients. 68 cells from 5 *Speg*$^{f/f}$ mice and 90 cells from 6 *Speg*$^{f/f}$/Myh6-MCM mice were analyzed.

C. Calcium transients elicited by electrical stimulation in primary cardiomyocytes isolated from the *Speg*$^{f/f}$ and *Speg*$^{f/f}$/Myh6-MCM mice at 6 weeks after tamoxifen induction. Amplitudes, full duration at half maximum (FDHM) and time constant Tau of calcium transients from 93 *Speg*$^{f/f}$ cells (5 mice) and 63 *Speg*$^{f/f}$/Myh6-MCM cells (5 mice), respectively.

D. SR calcium load in primary cardiomyocytes isolated from the *Speg*$^{f/f}$ and *Speg*$^{f/f}$/Myh6-MCM mice at 4 or 6 weeks after tamoxifen induction. The time constant Tau of caffeine-induced Ca^{2+} transients was shown for 6weeks after induction. 17 *Speg*$^{f/f}$ and *Speg*$^{f/f}$/Myh6-MCM cells were used in the assay at 4 weeks after induction. 27 *Speg*$^{f/f}$ cells and 16 *Speg*$^{f/f}$/Myh6-MCM cells were analyzed at 6 weeks after induction.

E-F. Calcium sparks in primary cardiomyocytes isolated from the *Speg*$^{f/f}$ and *Speg*$^{f/f}$/Myh6-MCM mice at 4 or 6 weeks after tamoxifen induction. Calcium spark frequency was analyzed in 24 cells of 3 *Speg*$^{f/f}$ mice and 27 cells of 3 *Speg*$^{f/f}$/Myh6-MCM mice at 4 weeks (E), and 39 cells of 4 *Speg*$^{f/f}$ mice and 40 cells of 4 *Speg*$^{f/f}$/Myh6-MCM mice at 6 weeks (F). Amplitudes, full duration at half maximum (FDHM) and time constant Tau of calcium sparks were analyzed in 275 sparks in *Speg*$^{f/f}$ cells and 298 sparks in *Speg*$^{f/f}$/Myh6-MCM cells at 4 weeks (E), and 1143 sparks in *Speg*$^{f/f}$ cells and 847 sparks in *Speg*$^{f/f}$/Myh6-MCM cells at 6 weeks (F).

The data in the bar graphs are given as the mean ± SEM. The bars in the scatter plots show the mean ± SEM. * indicates $p < 0.05$, ** indicates $p < 0.01$, and *** indicates $p < 0.001$.

Novelty and Significance

What is known?

- Calcium re-uptake into the sarcoplasmic reticulum (SR) through sarcoplasmic/endoplasmic reticulum calcium ATPase 2a (SERCA2a) is a pivotal process for heart function, whose dysregulation is directly linked to cardiomyopathy and heart failure.
- Striated muscle preferentially expressed protein kinase (SPEG) that has two kinase domains is a critical factor regulating heart development and cardiac function.
- The molecular mechanisms how SPEG functions to maintain cardiac performance remain largely unknown.

What new information does this article contribute?

- The second kinase domain of SPEG interacts with SERCA2a and phosphorylates the latter on Thr^{484}.
- Thr^{484} phosphorylation promotes oligomerization of SERCA2a and enhances its activity for calcium re-uptake into the SR.
- Knockout of SPEG decreases Thr^{484} phosphorylation of SERCA2a and prolongs calcium re-uptake into the SR, which leads to the development of heart failure.

SPEG deficiency causes dilated cardiomyopathy and heart failure in human patients as well as in mouse models, heightening the needs to elucidate the underlying mechanisms. In this study, we identified SERCA2a as a protein phosphorylation substrate for the second kinase domain of SPEG. SPEG-mediated phosphorylation of SERCA2a promotes its oligomerization and enhances its activity for calcium re-uptake into the SR. SPEG deficiency in cardiomyocytes decreases SERCA2a phosphorylation and delays calcium re-uptake into the SR, which leads to the development of heart failure. Our findings suggest that SPEG may serve as a new target to modulate SERCA2a activity for treatment of heart diseases with impaired calcium homeostasis.

Figure 1

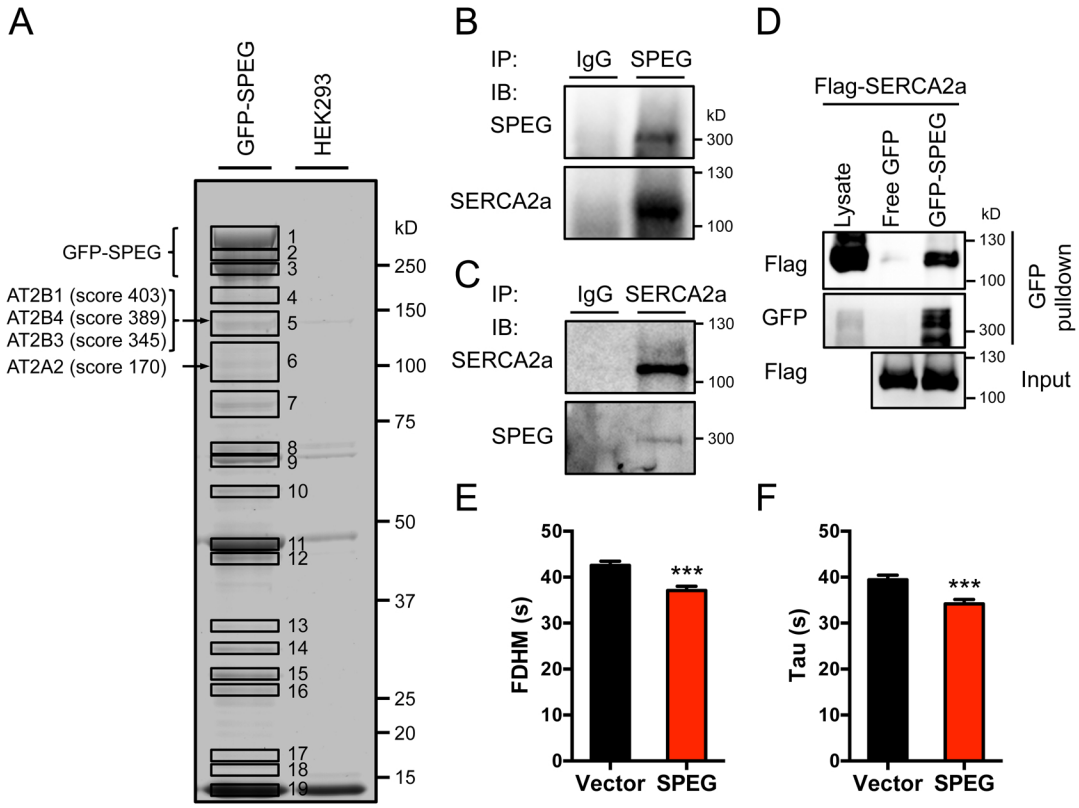
A
GFP-SPEG
HEK293
kD
250
150
100
75
50
37
25
20
15
GFP-SPEG
AT2B1 (score 403)
AT2B4 (score 389)
AT2B3 (score 345)
AT2A2 (score 170)
1
2
3
4
5
6
7
8
9
10
11
12
13
14
15
16
17
18
19
B
IP:
IgG
SPEG
IB:
SPEG
SERCA2a
kD
300
130
100
C
IP:
IgG
SERCA2a
IB:
SERCA2a
SPEG
130
100
300
D
Flag-SERCA2a
Lysate
Free GFP
GFP-SPEG
kD
Flag
GFP
Flag
130
100
300
130
100
GFP pulldown
Input
E
FDHM (s)
50
40
30
20
10
0
***
Vector
SPEG
F
Tau (s)
50
40
30
20
10
0
***
Vector
SPEG

Figure 2

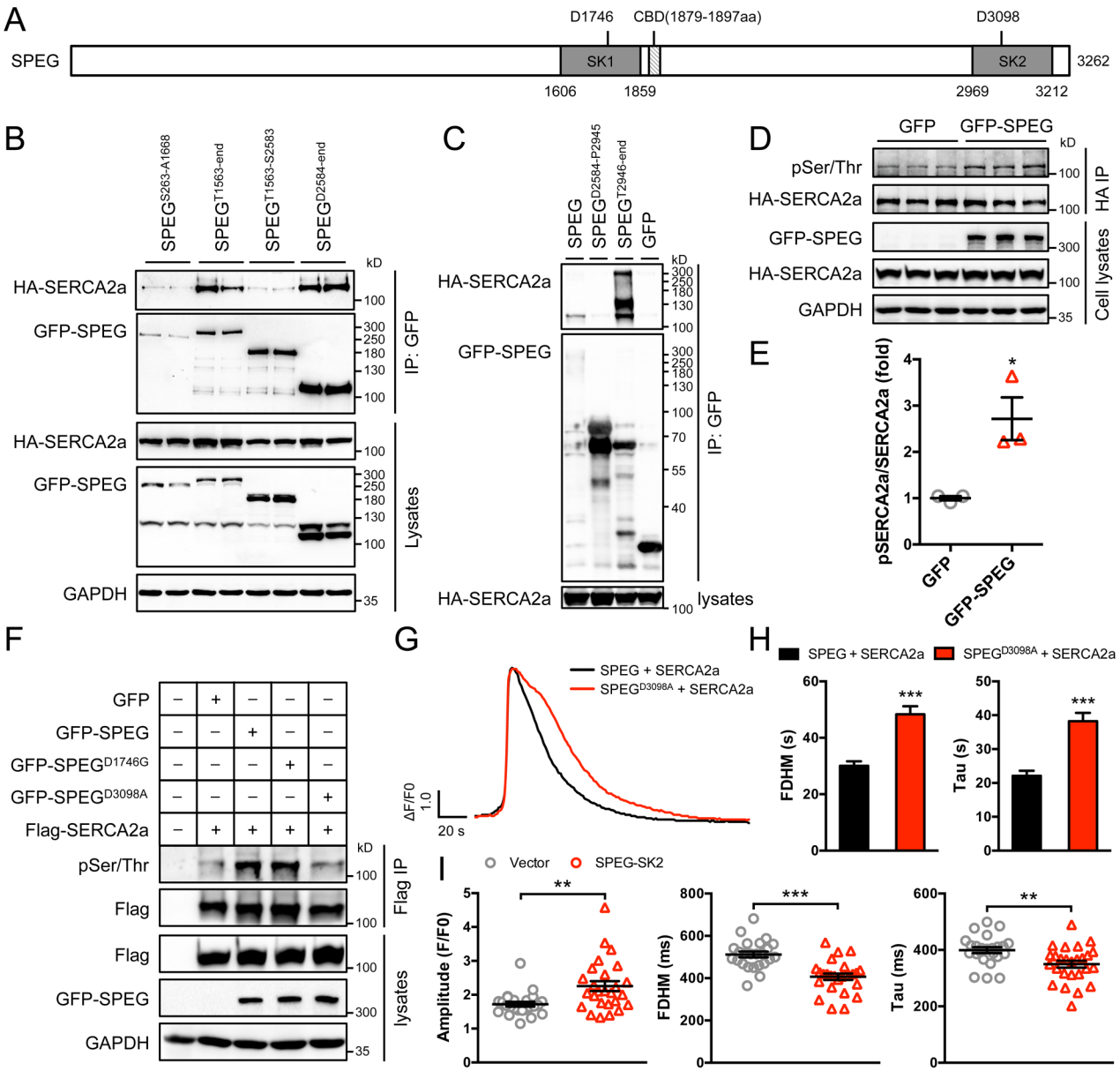
A
SPEG
D1746
CBD(1879-1897aa)
D3098
SK1
SK2
3262
1606
1859
2969
3212
B
SPEGS263-A1668
SPEGT1563-end
SPEGT1563-S2583
SPEGD2584-end
kD
HA-SERCA2a
GFP-SPEG
IP: GFP
Lysates
GAPDH
C
SPEG
SPEGD2584-P2945
SPEGT2946-end
GFP
IP: GFP
lysates
D
GFP
GFP-SPEG
pSer/Thr
HA IP
Cell lysates
E
pSERCA2a/SERCA2a (fold)
F
GFP-SPEGD1746G
GFP-SPEGD3098A
Flag-SERCA2a
Flag IP
Flag
lysates
G
SPEG + SERCA2a
SPEGD3098A + SERCA2a
ΔF/F0
20 s
H
FDHM (s)
Tau (s)
I
Vector
SPEG-SK2
Amplitude (F/F0)
FDHM (ms)
Tau (ms)

Figure 3

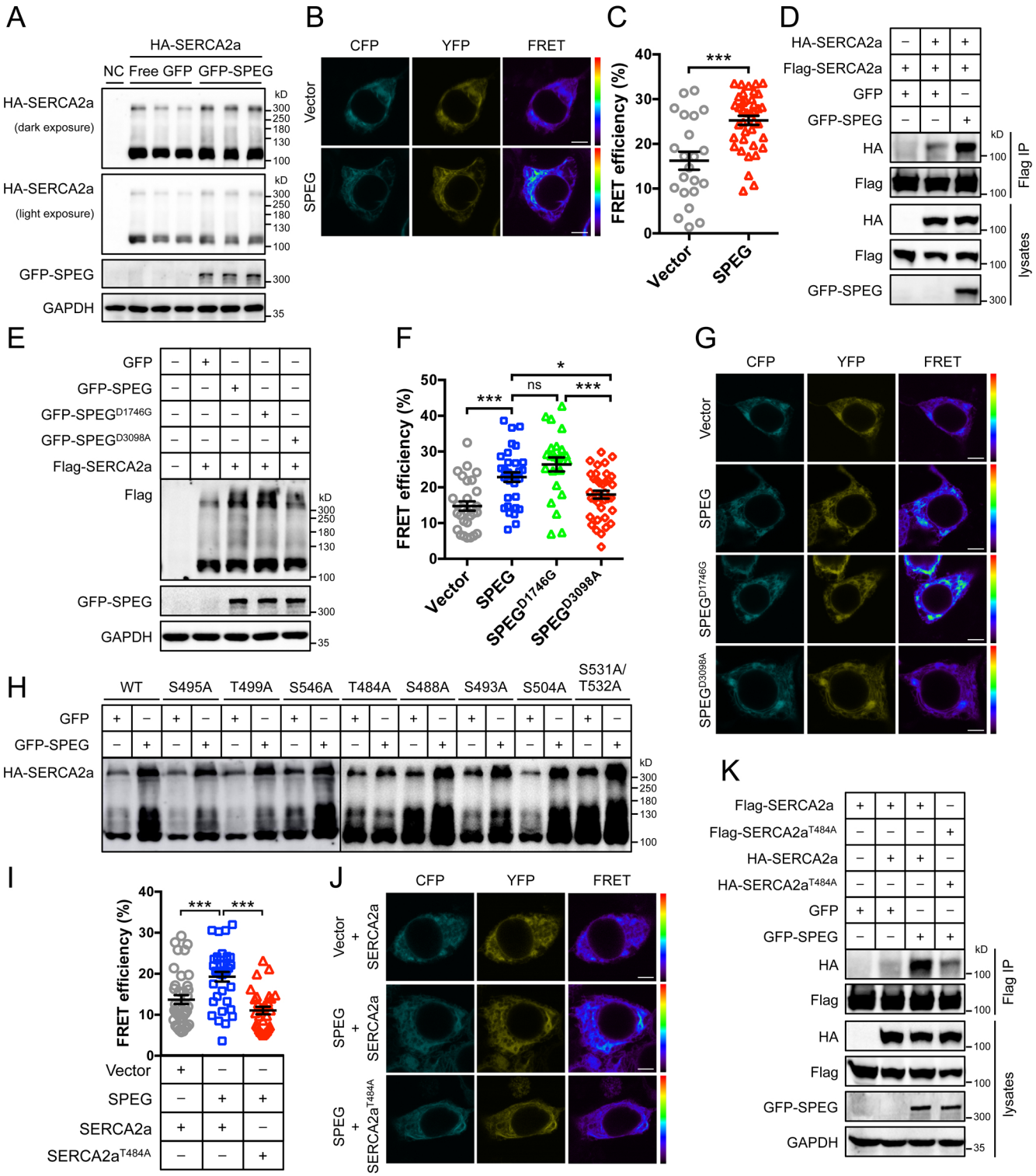
A
HA-SERCA2a
NC Free GFP GFP-SPEG
HA-SERCA2a (dark exposure)
HA-SERCA2a (light exposure)
GFP-SPEG
GAPDH
kD
300
250
180
130
100
35
B
CFP
YFP
FRET
Vector
SPEG
C
FRET efficiency (%)
***
Vector
SPEG
D
HA-SERCA2a
Flag-SERCA2a
GFP
GFP-SPEG
HA
Flag
Flag IP
lysates
E
GFP
GFP-SPEG
GFP-SPEG^{D1746G}
GFP-SPEG^{D3098A}
Flag-SERCA2a
Flag
GFP-SPEG
GAPDH
F
FRET efficiency (%)
***
ns
*
***
Vector
SPEG
SPEG^{D1746G}
SPEG^{D3098A}
G
CFP
YFP
FRET
Vector
SPEG
SPEG^{D1746G}
SPEG^{D3098A}
H
WT
S495A
T499A
S546A
T484A
S488A
S493A
S504A
S531A/ T532A
GFP
GFP-SPEG
HA-SERCA2a
kD
I
FRET efficiency (%)
***
***
Vector
SPEG
SERCA2a
SERCA2a^{T484A}
J
CFP
YFP
FRET
Vector + SERCA2a
SPEG + SERCA2a
SPEG + SERCA2a^{T484A}
K
Flag-SERCA2a
Flag-SERCA2a^{T484A}
HA-SERCA2a
HA-SERCA2a^{T484A}
GFP
GFP-SPEG
HA
Flag
Flag IP
HA
Flag
GFP-SPEG
GAPDH
lysates

Figure 4

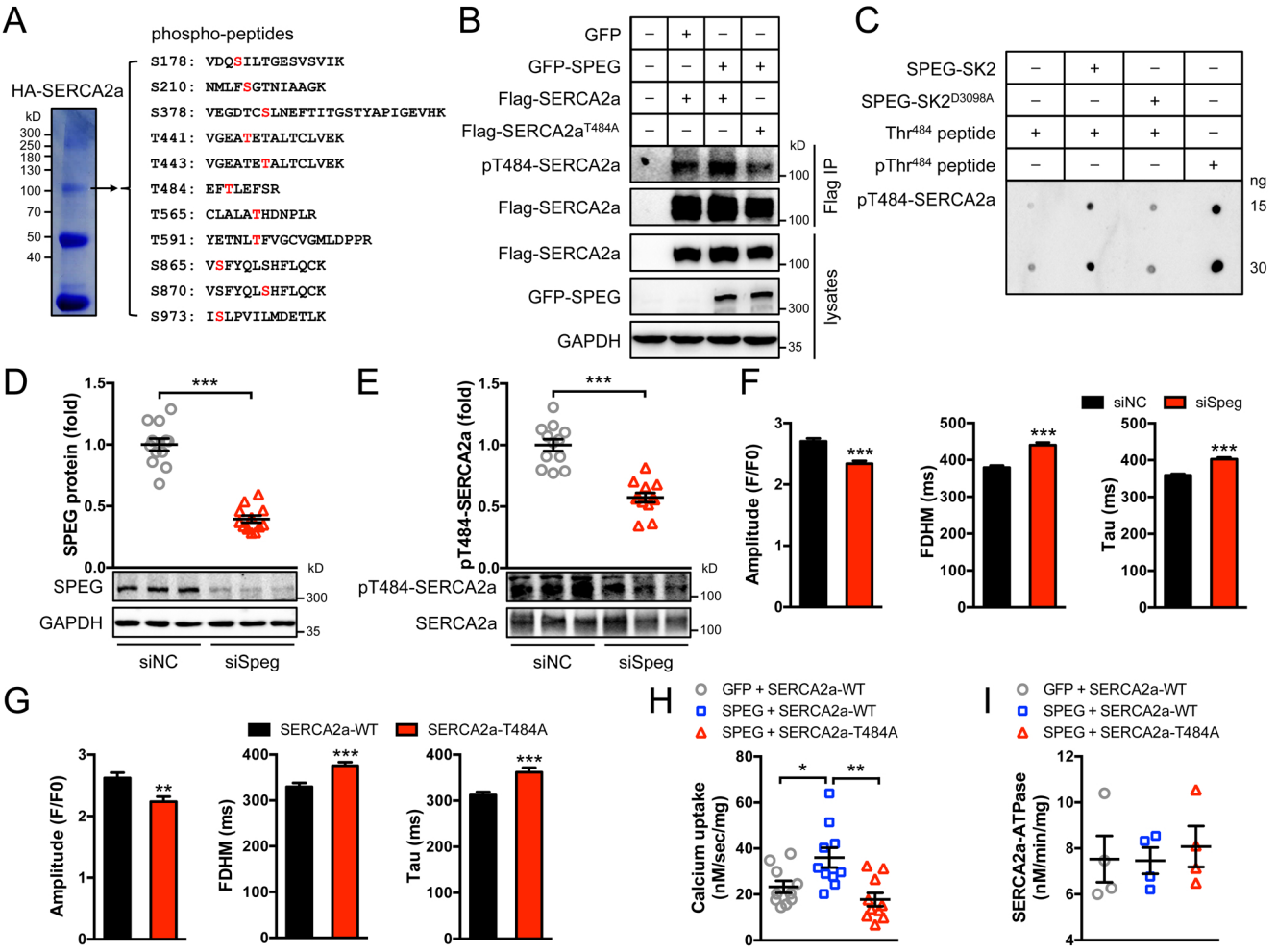
A
phospho-peptides
HA-SERCA2a
kD
300
250
180
130
100
70
50
40
S178: VDQSILTGESVSVIK
S210: NMLFSGTNIAAGK
S378: VEGDTCSLNEFTITGSTYAPIGEVHK
T441: VGEATETALTCLVEK
T443: VGEATETALTCLVEK
T484: EFTLEFSR
T565: CLALATHDNPLR
T591: YETNLTFVGCVGMLDPPR
S865: VSFYQLSHFLQCK
S870: VSFYQLSHFLQCK
S973: ISLPVILMDETLK
B
GFP
GFP-SPEG
Flag-SERCA2a
Flag-SERCA2a^T484A
pT484-SERCA2a
Flag-SERCA2a
Flag-SERCA2a
GFP-SPEG
GAPDH
kD
100
100
100
300
35
Flag IP
lysates
C
SPEG-SK2
SPEG-SK2^D3098A
Thr^484 peptide
pThr^484 peptide
pT484-SERCA2a
ng
15
30
D
SPEG protein (fold)
***
SPEG
GAPDH
kD
300
35
siNC
siSpeg
E
pT484-SERCA2a (fold)
***
pT484-SERCA2a
SERCA2a
kD
100
100
siNC
siSpeg
F
siNC
siSpeg
Amplitude (F/F0)
FDHM (ms)
Tau (ms)
***
G
SERCA2a-WT
SERCA2a-T484A
Amplitude (F/F0)
FDHM (ms)
Tau (ms)
**
***
H
GFP + SERCA2a-WT
SPEG + SERCA2a-WT
SPEG + SERCA2a-T484A
Calcium uptake (nM/sec/mg)
*
**
I
GFP + SERCA2a-WT
SPEG + SERCA2a-WT
SPEG + SERCA2a-T484A
SERCA2a-ATPase (nM/min/mg)

Figure 5

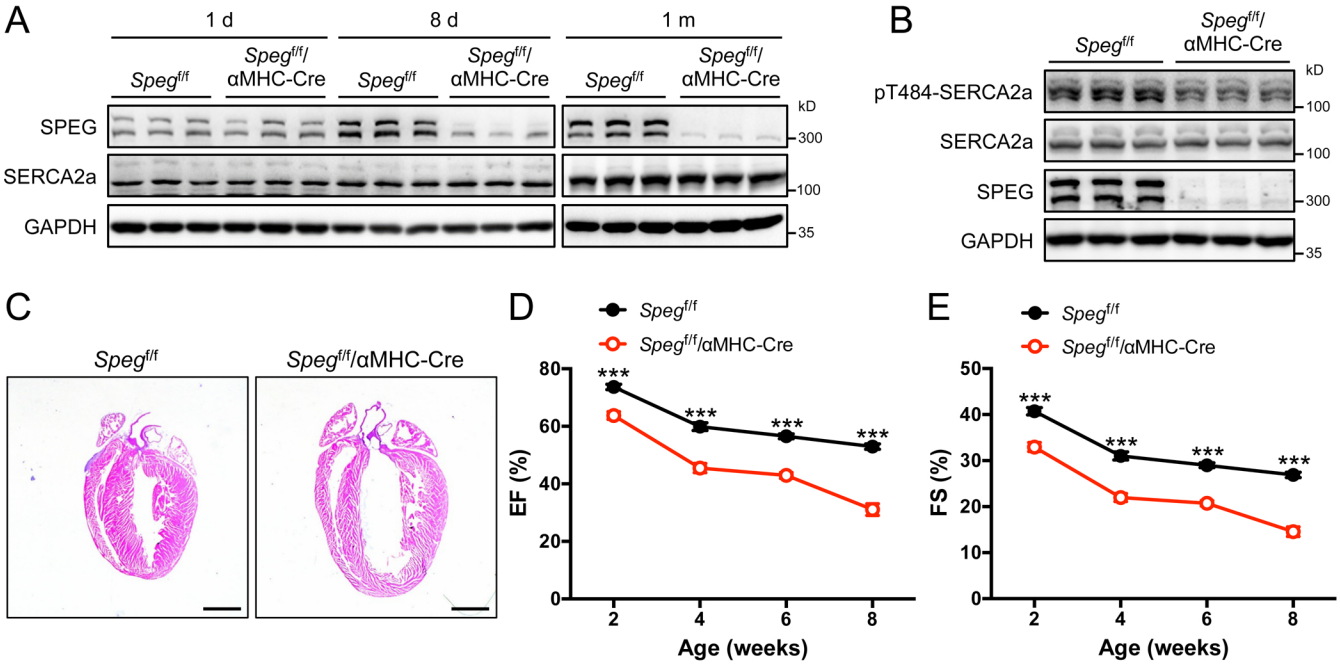
A
1 d
8 d
1 m
Speg f/f
Speg f/f/ αMHC-Cre
SPEG
SERCA2a
GAPDH
kD
300
100
35
B
pT484-SERCA2a
SERCA2a
SPEG
GAPDH
kD
100
100
300
35
C
Speg f/f
Speg f/f/αMHC-Cre
D
Speg f/f
Speg f/f/αMHC-Cre
EF (%)
Age (weeks)
***
E
Speg f/f
Speg f/f/αMHC-Cre
FS (%)
Age (weeks)
***

Figure 6

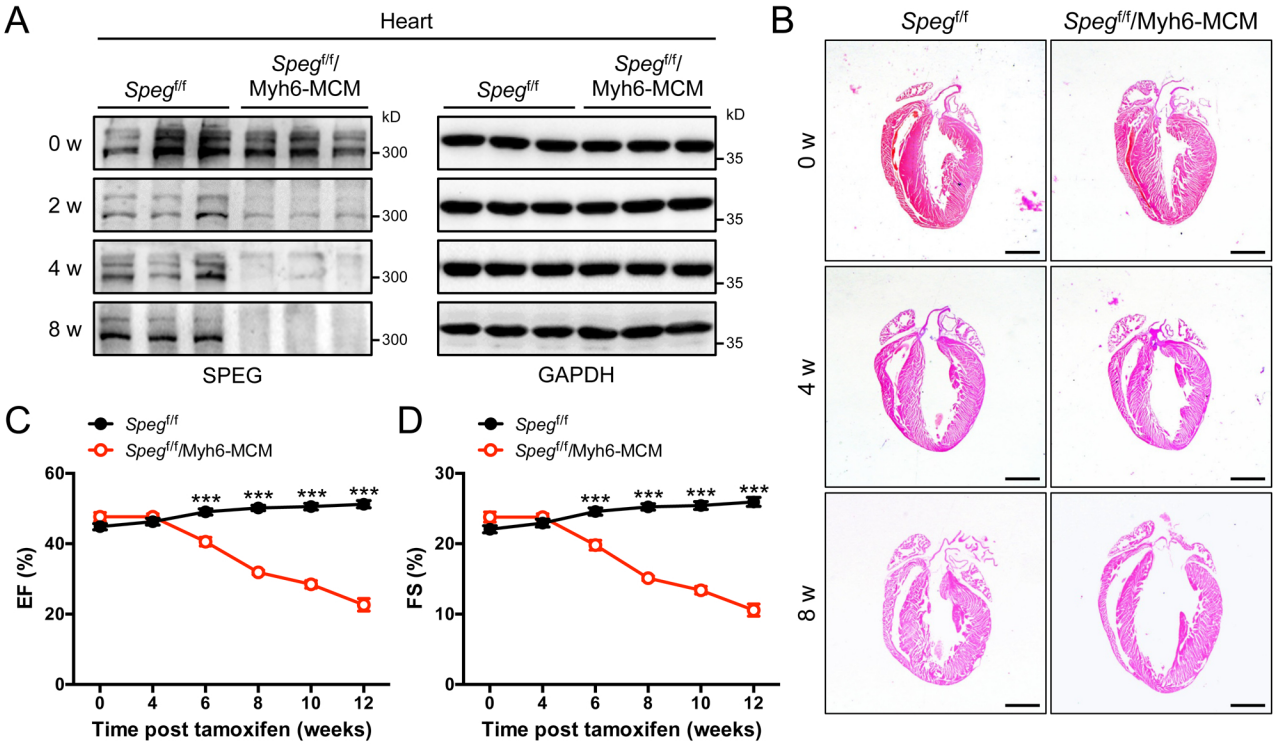
A
Heart
Speg f/f
Speg f/f/ Myh6-MCM
kD
0 w
2 w
4 w
8 w
300
35
SPEG
GAPDH
B
Speg f/f
Speg f/f/Myh6-MCM
0 w
4 w
8 w
C
Speg f/f
Speg f/f/Myh6-MCM
EF (%)
Time post tamoxifen (weeks)
***
D
FS (%)
Time post tamoxifen (weeks)

Figure 7

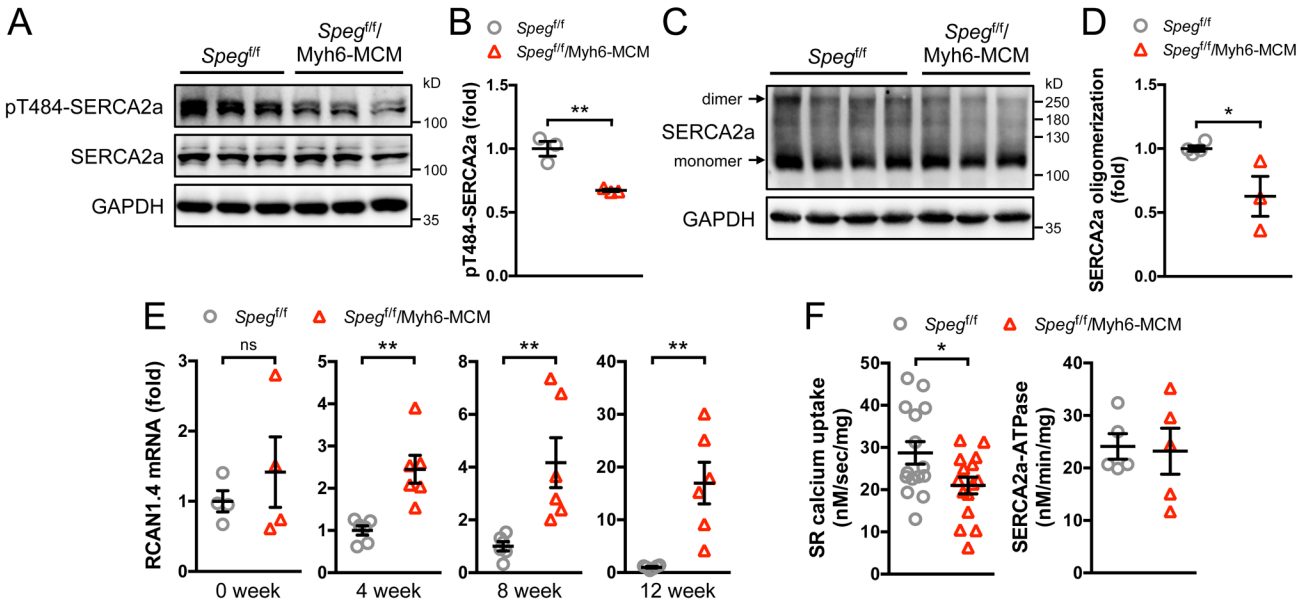
A
Speg f/f
Speg f/f/ Myh6-MCM
kD
pT484-SERCA2a
100
SERCA2a
100
GAPDH
35
B
Speg f/f
Speg f/f/Myh6-MCM
pT484-SERCA2a (fold)
1.5
1.0
0.5
0.0
**
C
Speg f/f
Speg f/f/ Myh6-MCM
kD
dimer
SERCA2a
monomer
250
180
130
100
GAPDH
35
D
Speg f/f
Speg f/f/Myh6-MCM
SERCA2a oligomerization (fold)
1.5
1.0
0.5
0.0
*
E
Speg f/f
Speg f/f/Myh6-MCM
RCAN1.4 mRNA (fold)
ns
**
**
**
0 week
4 week
8 week
12 week
F
Speg f/f
Speg f/f/Myh6-MCM
SR calcium uptake (nM/sec/mg)
*
SERCA2a-ATPase (nM/min/mg)

Figure 8

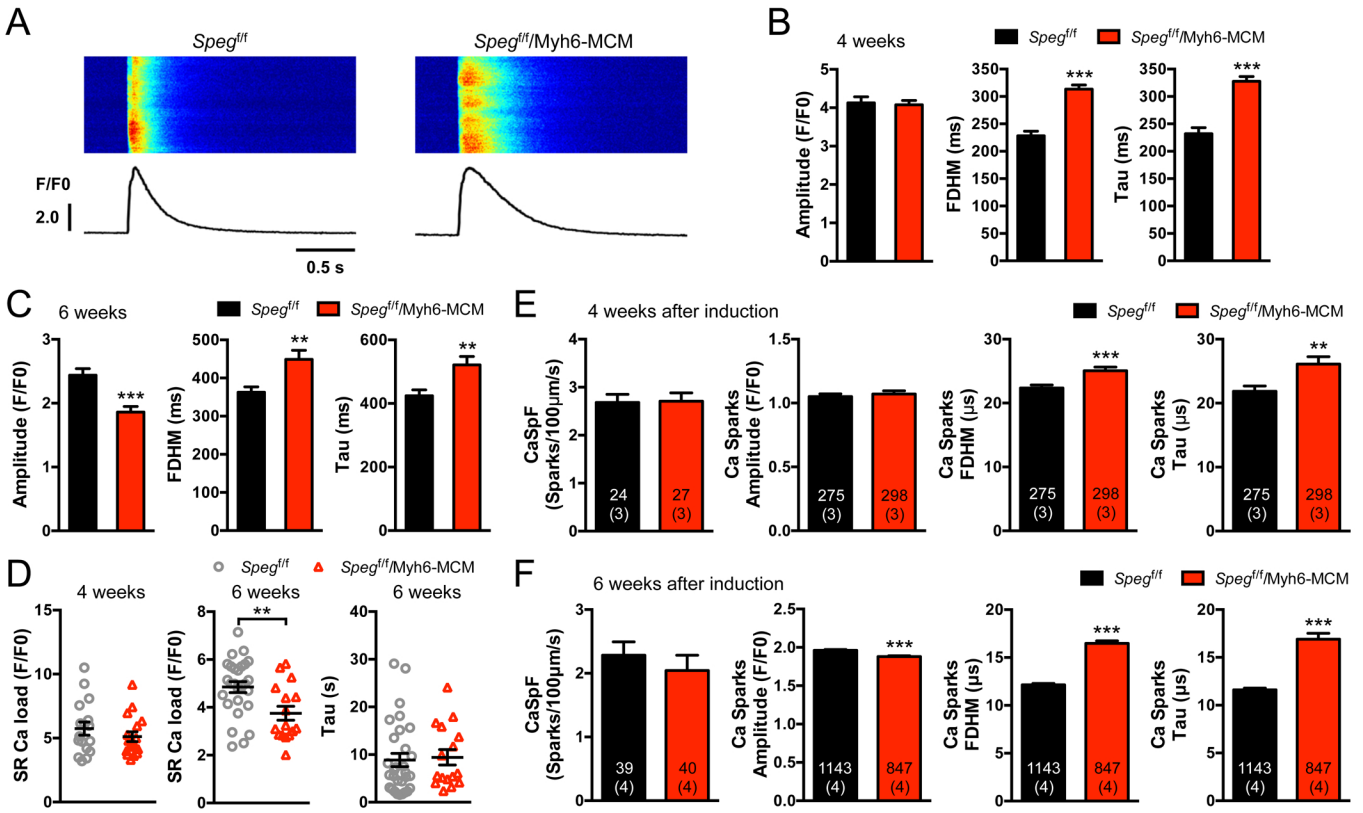
A
Speg f/f
Speg f/f/Myh6-MCM
F/F0
2.0
0.5 s
B
4 weeks
Speg f/f
Speg f/f/Myh6-MCM
Amplitude (F/F0)
FDHM (ms)
Tau (ms)
***
C
6 weeks
Amplitude (F/F0)
FDHM (ms)
Tau (ms)
**
***
D
4 weeks
6 weeks
6 weeks
SR Ca load (F/F0)
SR Ca load (F/F0)
Tau (s)
**
E
4 weeks after induction
CaSpF (Sparks/100µm/s)
Ca Sparks Amplitude (F/F0)
Ca Sparks FDHM (µs)
Ca Sparks Tau (µs)
24 (3)
27 (3)
275 (3)
298 (3)
F
6 weeks after induction
CaSpF (Sparks/100µm/s)
Ca Sparks Amplitude (F/F0)
Ca Sparks FDHM (µs)
Ca Sparks Tau (µs)
39 (4)
40 (4)
1143 (4)
847 (4)